CHAPTER IV
NANOCLAY/POLYPROPYLENE NANOCOMPOSITE DYED FIBER

4.1 ABSTRACT

Nowadays, polypropylene is widely used in fiber industry because of its advantages such as low density, good chemical resistance, easy processibility, good surface resistance, strain resistance and especially it has low cost which is the advantage over nylon and polyester fibers. However, polypropylene has some drawbacks relating to its dye–ability due to its non polar aliphatic structure and high crystallinity; it does not have active sites to attach with functional groups of dyes, resulting in poor dyeability. In this study, the organoclay was incorporated into polypropylene (PP) fiber to act as a dye sorption part for improving the dyeability of the fiber. The dyeability of organoclay–polypropylene fibers extruded at different draw ratios was investigated, as well as those with different surfactant modified–nanoclays. Result from the K/S (the color intensity) showed that the PP fiber modified with 5 phr organoclay can absorb dye molecules better than the unfilled fiber because adding organoclay causes an enhancement in the polar group and active sites for the dye molecules. In addition, fiber modified with 5 phr BTC–organoclay showed better dye absorption than DOEM–organoclay because the aromatic groups in the BTC–organoclay is more significant than polar groups of the DOEM–organoclay. Among acid, basic, disperse, and direct dyes, the disperse dye is the best dye that can be absorbed on the organoclay/PP fiber, and much better than the unfilled fiber. Moreover, its absorption is better than other types of dye. The dye absorption of modified fibers increased with amount of organoclay.

Keywords : nanoclay–polypropylene fiber, dyed fiber

4.2 INTRODUCTION

Polypropylene is widely used in fiber industry because of its advantages such as low density, good chemical resistant, easy processibility, good surface resistance, strain resistance and especially it has low cost which is the advantage over

nylon and polyester fibers. However, polypropylene presents some drawback due to the structure of polypropylene which is non polar aliphatic structure and has high crystallinity. So it does not have active site to attach with functional group of dyes and results in poor dyeability. Articles made from polypropylene usually colored by pigments. However, the use of pigments is not trivial and often has a deleterious effect on other properties of fibers. In addition, the pigment must be added to the polymer while polymer is molten and the process for producing fiber need to be done again if changing of the color is required. So this is very inconvenient for the fiber industry. Due to this problem, the improvement of dyeability of polypropylene is needed to achieve fiber that can be easily dyed by the conventional process in fiber industry.

The poor dyeability problem of polypropylene can be solved by addition of the active groups that will form interactions with dye molecules. There are various methods for producing polypropylene with active sites to improve dyeability such as copolymerization with other monomers[4], blending or grafting with other polymers [6], [7] or metal complex or use of additives. However, all of these technologies result in the higher cost of products and the manufacturing cost is no longer an outstanding property of polypropylene over nylon and polyester.

Another and a more recent method for producing dyeable polypropylene is the addition of nanoparticles into polymer to act as dye sorption [11-13]. This method is better than the previous methods. The improvement of dyeability by chemical reaction requires chemical reactivity in polymer structure but it does not necessary for the use of nanoparticles. And due to its small size that give large surface area that necessary for a good sorbent so nanoparticles can be used to improve dyeability in polypropylene and also improve other properties of textiles. Nanoclay is interested over other particles because of its common availability with good quality and low price.

In the present study, the dyeability of polypropylene fiber was improved by the use of organo–modified clay. The nanoclay/polypropylene fiber was prepared and its dyeability was investigated. Dyeability of the fiber with various types of dye i.e. acid dye, basic dye, disperse dye and direct dye, and organoclay with different

types of modifying agents were studied. Also, the amount of clay and draw ratio for producing polypropylene nanoclay fiber were optimized.

4.3 EXPERIMENTAL

Polypropylene (MFI 11 dg/min) was obtained from IRPC Co., Ltd. Thailand under trade name polypropylene NK1126.

Commercial sodium activated bentonite Mac-Gel® (GRADE SAC), Na-BTN, with cationic exchange capacity (CEC) of 44.3 meq/100 g clay, was supplied by Thai Nippon Co., Ltd. Thailand.

Methyl di-[(partially hydrogenated) tallow carboxyethyl]-2-dihydroxyethyl ammonium methyl sulfate (DOEM) was received from Union Compound Co., Ltd. N-alkyl dimethyl ammonium chloride (BTC 8358®) was obtained from Sunny World Co., Ltd.

Polypropylene grafted maleic anhydride (PP-g-MAH), Polybond®3200 (1 wt% MA grafted level) was purchased from Chemtula Co., Ltd. Thailand. Sodium-neutralized ethylene-co-methacrylic acid, Surlyn® PC350, 4.5 MFI was purchased from DuPont Co., Ltd.

Dyes that were used in this experiment are Lanaset Red 2B (acid dye), Maxilon Red GRL 200% (Basic dye), Terasil Red SD (Disperse dye), and Erionyl Red A-2BF (Direct dye). All types of dye were obtained from Ciba Co., Ltd.

Preparation of organo–modified clay

Preparation of organo-modified clay was carried out following the experiment procedure established by Sakkarin (2007). Na-Bentonite of 300 g was swollen in 1500 ml water for 24 hr. 100 g surfactant was dissolved in the 500 ml water at 80 °C for 30 min. The whole swollen clay suspension was mixed with the whole 500 ml surfactant solution in 5 L mixer and kept at 80 °C for 2 hr with vigorously stirring. After that the mixture was homogenized at 80 °C for 1 hr. The sediment was filtrated and washed with hot water several times to remove the excess salts until the washed water turn from basic to neutral. It was then dried in a vacuum

oven at 100 °C overnight. The dried sample was ground to powder and screened through a mesh #325.

Preparation of organo–modified clay/polypropylene nanocomposites

Preparation of organo-modified clay/polypropylene nanocomposites was also carried out based on procedure adapted by Sakkarin (2007). The polypropylene nanocomposites were prepared as a two-step compounding process. First, 60%wt organoclay was blended with 40%wt compatibilizers (PP-g-MAH and Surlyn®) using twin screw extruder as a masterbatch. The operating temperatures were maintained at 80/160/180/190/200/210°C with screw speed of 50 rpm. The masterbatch were dried in a vacuum oven at 80 °C for 12 hr for moisture removal. Then, the required amount masterbatch was mixed with polypropylene and compatibilizer pellets in a tumble dry mixer for 10 min, then the melt compounding of the premix was carried out by using a twin screw extruder to produce 3, 5, and 7 phr oganoclay/polypropylene nanocomposites. The operating temperatures were maintained at 80/160/180/190/200/210°C with screw speed of 50 rpm; the extrudate strand was cooled in a water bath and pelletized.

Spinning process

Before undergo melt spinning, the polypropylene and polypropylene/organoclay nanocomposite pellets were dried in a vacuum oven for 4 hr at 80 °C to remove any moisture on the polypropylene pellets. Melt spinning was performed at 190 °C on a melt spinning machine. Fibers were extruded with draw ratios of 15.3, 26.5, 36.6, and 47.6 (x1000).

Dyeing process

Fibers were dyed with acid, basic, disperse, and direct dye. Fiber samples were placed into a dye pot and placed in a dyeing machine (DAELIM Starlet model DL-6000). Temperature was raised to 50 °C 30 minutes and raised up to 100 °C. Temperature was kept constant at 100 °C for 60 min. Then, temperature was

decreased to 50 °C. Fiber was washed with water 30 min at room temperature and wash with tap water for 1 min.

Thermal analysis

TG-DTA curves were collected on a Perkin-Elmer Pyris Diamond TG/DTA instrument. The sample was loaded on the platinum pan and heated from 30°C to 700°C at a heating rate of 10°C/min under N_2 flow.

DSC analysis were carried out using a Perkin-Elmer DSC 7 instrument. The sample was first heated from 30°C to 200°C and cooled down at a rate of 10°C/min under a N_2 atmosphere with a flow rate of 60 ml/min. The sample was then reheated to 200°C at the same rate. The melting and crystallization temperature and the crystallinity can be determined by DSC. The crystallinity can be calculated with the following formula

$$\% \text{ crystallinity} = \frac{\Delta H_{sample}}{\Delta H^{0}_{pp}} \times 100$$

where ΔH = enthalpy of fusion of the sample (J/g)

ΔH = enthalpy of fusion of completely crystalline PP (~ 209 J/g) [15]

Physical analysis

X-ray diffraction patterns were measured on a Rigaku Model Dmax 2002 diffractometer with Ni-filtered Cu K_α radiation operated at 40 kV and 30 mA. The nanoconposite films were observed on the 2θ range of 1.5-30 degree with a scan speed of 2 degree/min and a scan step of 0.02 degree.

The crystal size can be determined by the Scherrer equation

$$L = K\lambda/B\cos\theta$$

Where L = average crystal size

K = full width at half maximum of the peak

Scanning electron microscopy was performed on JEOL JSM-6400 scanning electron microscope (SEM) and the Si species were identified by LINK ISIS series 300 for energy dispersive X-ray (EDX) analysis.

Scanning probe microscope was performed on Nanoscope IV scanning probe microscope by silicon probe with tapping mode.

Chemical Analysis

FT-IR spectra of PP and modified PP fiber were obtained using a Nicolet Nexus 670 FT-IR spectrometer in the frequency range of 4000-400 cm^{-1} with 128 scans at a resolution of 4 cm^{-1}. The spectra were recorded with the polarization radiation parallel and perpendicular to the draw direction to investigate the orientation of the fibers. The dichroic ratio and angle of orientation were calculated from the following equations.

$$\text{Dichroic ratio } D = A_{\parallel}/A_{\perp}$$

where $A_{\parallel}$ = Intensity of light polarized parallel to fiber axis after passing through the material

$A_{\perp}$ = Intensity of light polarized perpendicular to fiber axis after passing through the material

$$D_0 = 2\cot^2\alpha$$

where D_o = the value of the dichroic ratio corresponding to a perfectly oriented sample

α = angle between the transition moment of vibration of this group and the axis of the polymer chain

$$f = \frac{(D-1)}{(D+2)}\frac{(D_0+1)}{(D_0-2)}$$

$$f = \overline{(3\cos^2\theta - 1)/2}$$

where f = Herman Orientation Function

Tensile Testing

Polypropylene-organoclay nanocomposite fibers were tested mechanical properties with Lloyd Universal Testing 4206 by follow ASTM D3822-01. Crosshead speed is 290 mm/min. Linear density of polypropylene fibers were ranged from $1.85x10^5$ to $6.58x10^6$ tex dependent on draw ratio from 15..$x10^3$ to $47.6x10^3$. The gauge length is 20 mm. Each sample was tested for 10 times.

Color analysis

Dye solutions left in the dye baths before and after dyeing process were used to determine the content of % dye exhaustion by UV-Visible absorption. For the acid, basic direct, and disperse dyes, the absorbance were measure at wavelength 525, 530, 500, and 490 nm (which are λ_{max} of acid, basic, direct, and disperse dye) respectively.

$$\% \text{ Dye exhaustion} = \frac{(C_f - C)_i}{C_i} x100$$

Where C_i = concentration of dye solution before dyeing process

C_f = concentration of dye solution after dyeing process

The color intensity of fiber was measured by reflectance mode of UV-Visible Absorption. K/S (absorption to scattering coefficient) values of dyed samples were calculated by the measuring their reflectance (R) in visible spectrum (200-800 nm).

$$K/S = (1-R)^2/2R$$

Where K/S = absorption to scattering coefficient

R = reflectance

Color intensity can be also measured by Chromameter. The color intensity was represent by the following parameters and equation.

$$\Delta E = \sqrt{\Delta L^{2*} + \Delta a^{2*} + \Delta b^{2*}}$$

Where

ΔE = The difference in color (Eab) between any two points in the color space

Δ L* = The brightness difference between sample and control sample

Δ a* = The redness difference between sample and control sample

Δ b* = The yellowness difference between sample and control sample

Wash fastness of the fiber was determined according to ISO 105 C01-C03 which was carried out at 60 °C. The fibers were washed in the washing machine at the rotational frequency 40 rounds/min for 30 minutes. The changing color was determined by comparing with the standard gray scale.

4.4 RESULT AND DISSCUSSION

4.4.1 Characterization of Organo-modified clay/PP nanocomposite fibers

Crystal structure of polypropylene (PP) and organoclay/polypropylene nanocomposites fibers was investigated by XRD with 2θ ranging from 1.5 to 30°. According to the XRD patterns of BTC–organoclay/PP and DOEM–organoclay/PP are shown in Fig. 4.1-4.3. The peak at 5.7° was observed for BTC/PP fiber and peak at 6.12° for DOEM/PP fiber. The interlayer spacing for the two fibers were calculated according to the Bragg equation to be 1.54 nm for BTC/PP fiber and 1.45 nm for DOEM/PP fiber which was indicated that polypropylene can penetrate in to the BTC organoclay layer better than DOEM organoclay layer. Since there is no change in the peak position of polypropylene crystal, the results indicated that organoclay could be intercalated into PP resin with no influence on the crystal structure of polypropylene [14]. The crystal size of (130) plane of polypropylene crystal of polypropylene and organoclay/polypropylene nanocomposite fibers with different draw ratio were determined by Scherrer equation. The result showed that the fibers extruded with lower draw would be smaller than the crystal size of the fiber produced with the higher draw. These indicated that higher draw ratio induced a variation in growing habit of polypropylene crystals (Table 4.1) [15].

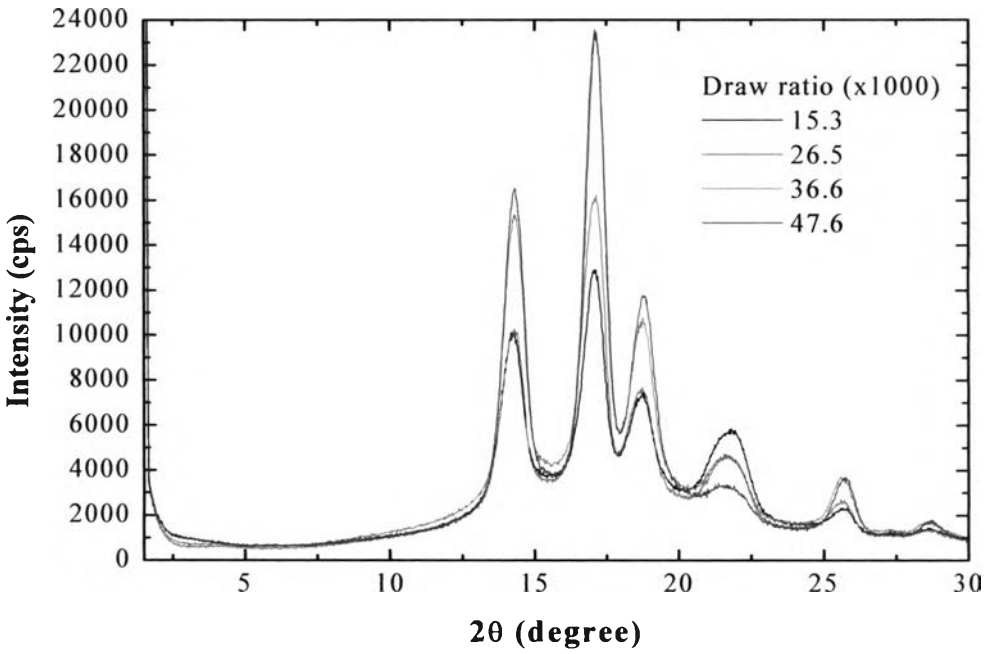

Figure 4.1 XRD patterns of PP fiber with various draw ratio

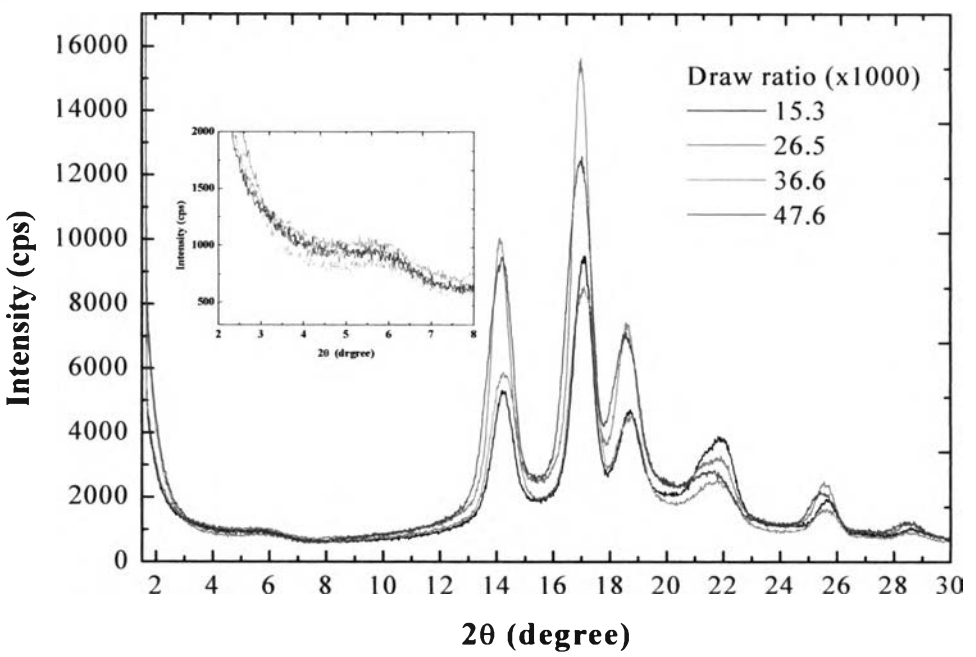

Figure 4.2 XRD patterns of BTC/PP fiber with various draw ratio

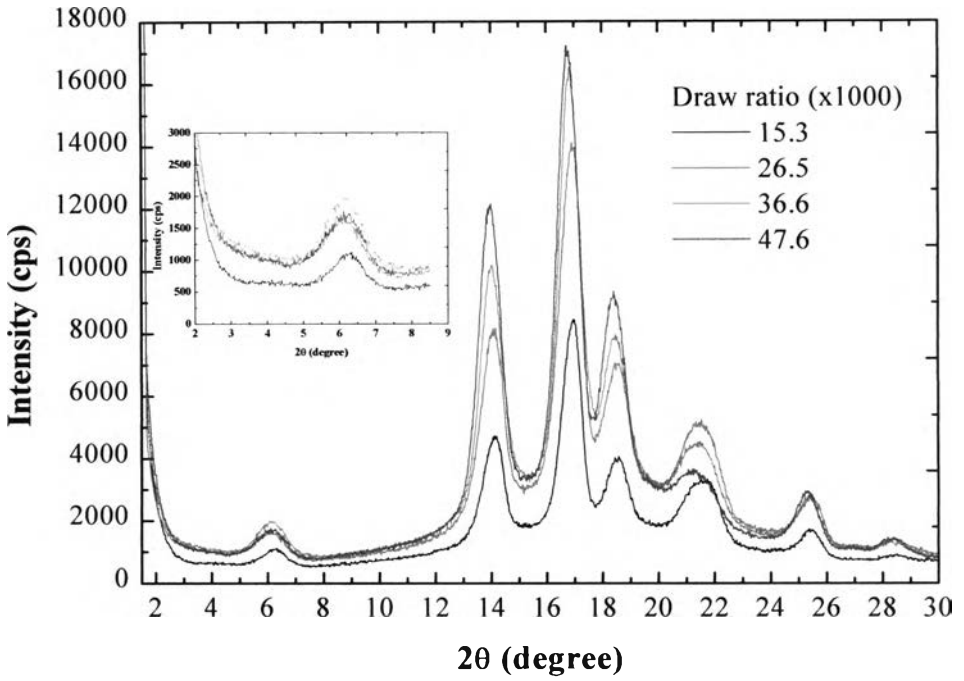

Figure 4.3 XRD patterns of DOEM/PP fiber with various draw ratio

Table 4.1 Crystal size of (130) plane of polypropylene and organoclay/ polypropylene nanocomposite fibers at various draw ratio

Samples	Draw ratio (x1000)	FWHT	Crystal size (nm)
PP	15.3	0.329	0.444
	26.5	0.235	0.622
	35.6	0.212	0.689
	47.6	0.141	1.036
5 phr BTC/Sur/PP	15.3	0.447	0.327
	26.5	0.329	0.444
	35.6	0.165	0.885
	47.6	0.165	0.885
5 phr DOEM/Sur/PP	15.3	0.588	0.248
	26.5	0.282	0.518
	35.6	0.165	0.885
	47.6	0.118	1.238

4.4.2 Thermal Analysis of Nanoclay/Polypropylene Nanocomposite Fiber

Introduction of organoclay to polypropylene caused an increase in the degradation temperature of nanocomposite fibers because organoclay is an inorganic material which has high degradation temperature. From TGA curves (Fig. 4.4-4.5), onset temperature of PP fiber was 426 °C, while the onset temperature of organoclay–PP nanocomposite fibers were induced to 429 °C (5phr BTC/Surlyn/PP), 438.5 °C (7 phr DOEM/Surlyn/PP) (Table 4.2). However, 7 phr BTC/Surlyn/PP fiber showed the lower degradation temperature than PP fiber, probably due to the poor dispersion and aggregation of organoclay in polypropylene matrix.

Melting temperatures of PP and the nanocomposite fibers were measured by DSC heating scan thermograms. From Table 4.3 melting temperature of nanocomposite fibers were closed to that of polypropylene (see Figure 4.6 and 4.8). The result suggested that compatibilizer and organoclay gave minimal effect to the melting temperature of nanocomposite fibers. From DSC thermograms we also observed that polypropylene–clay nanocomposite fibers had higher crystallization temperatures and higher crystallinity than the neat polypropylene fiber (Fig. 4.7 and 4.9 and Table 4.4-4.5). This could be due to organoclays act as the nucleating agent for crystallization of the fibers. From Fig. 4.10 – 4.13 and Table 4.6, when the draw ratio of the fibers was increased, the crystallinity of the fibers were also increased because polymer chains would rearrange themselves in the drawing direction. The higher the draw ratio, the more order of the molecules and the easier the crystallization to occur. Moreover, increasing the draw ratio would result in higher T_c for PP fiber but hardly affects on T_c of the organoclay/PP fiber. On the other hand, melting temperature of PP fiber is hardly altered by increasing draw ratio but the melting temperature of organoclay/PP fiber increases with draw ratio, especially for 5 phr BTC/Surlyn/PP.

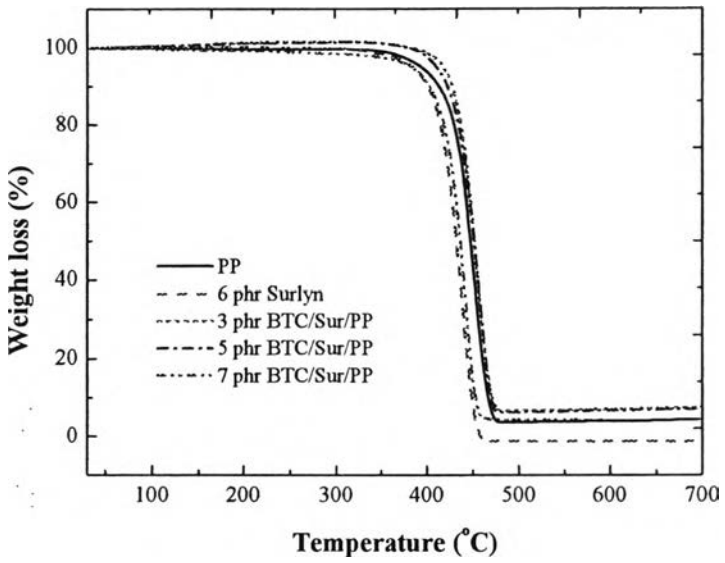

Figure 4.4 TG-DTA curves of unmodified and various amount of BTC-organoclay modified PP fibers.

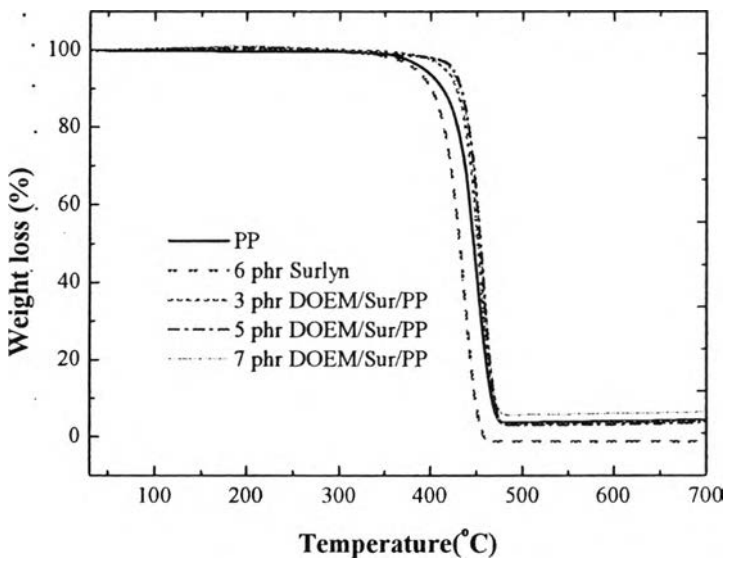

Figure 4.5 TG-DTA curves of unmodified and various amount of DOEM-organoclay modified PP fibers.

Table 4.2 Effect of amount and type of organoclay on the degradation temperature of the fibers

Samples	T_d onset (°C)	DTG (°C)
Polypropylene (PP)	426.0	452.1
6 phr Surlyn/PP	412.4	436.0
3 phr BTC/Surlyn/PP	431.9	455.5
5 phr BTC/Surlyn/PP	429.6	457.3
7 phr BTC/Surlyn/PP	418.3	442.1
3 phr DOEM/Surlyn/PP	434.4	455.8
5 phr DOEM/Sur/PP	438.5	458.3
7 phr DOEM/Surlyn/PP	438.5	458.1

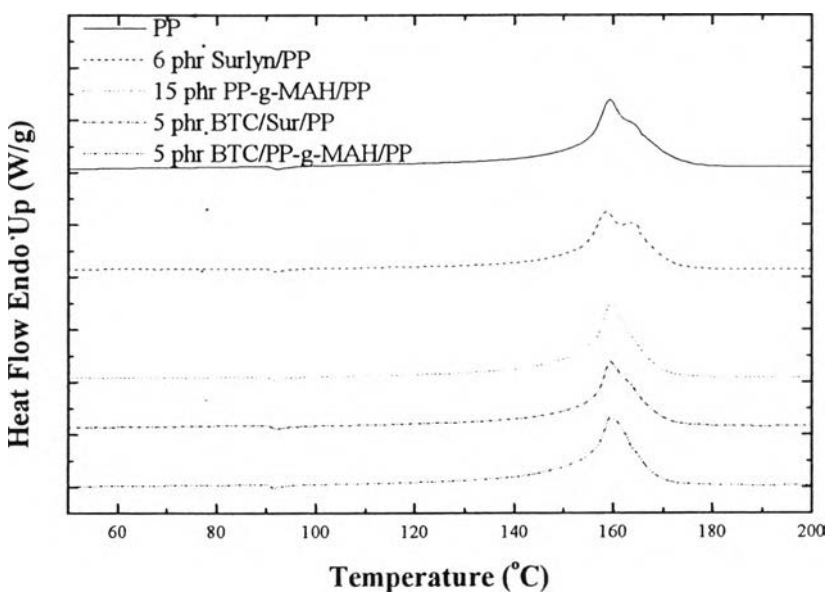

Figure 4.6 Effect of compatibilizers on the melting temperature (T_m) of the fibers

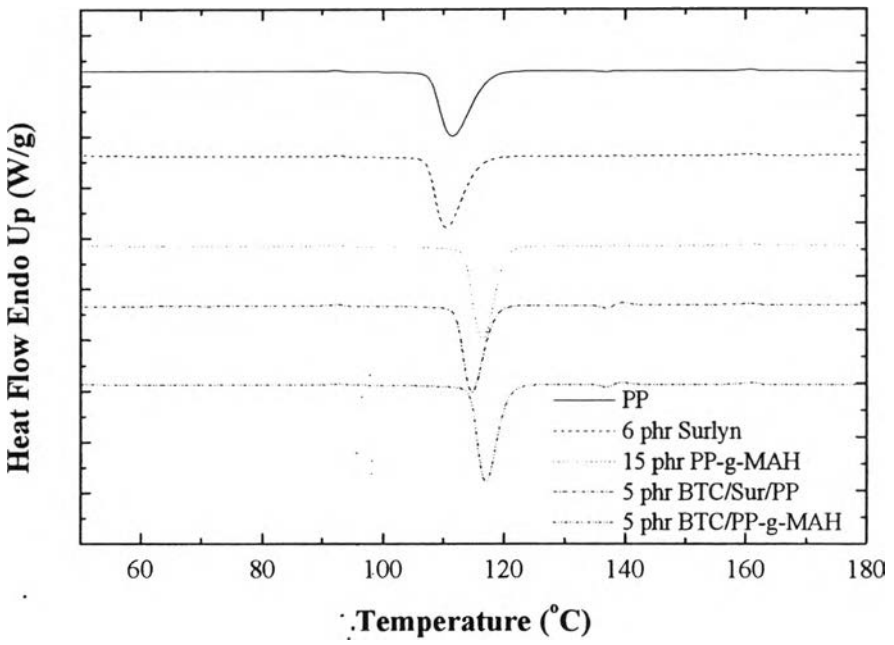

Figure 4.7 Effect of compatibilizers on the crystallization temperature (T_c) of the fibers

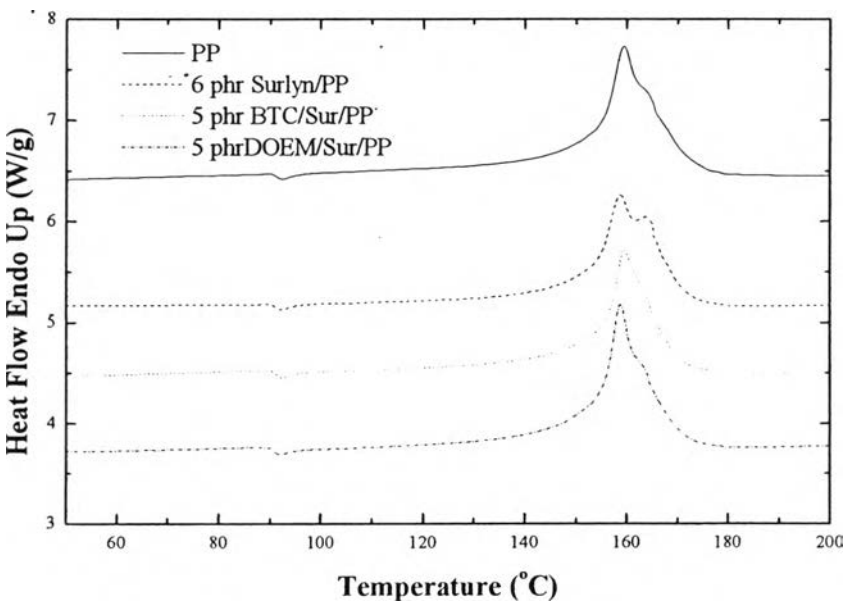

Figure 4.8 Effect of type of organoclay on the melting temperature (T_m) of the fibers

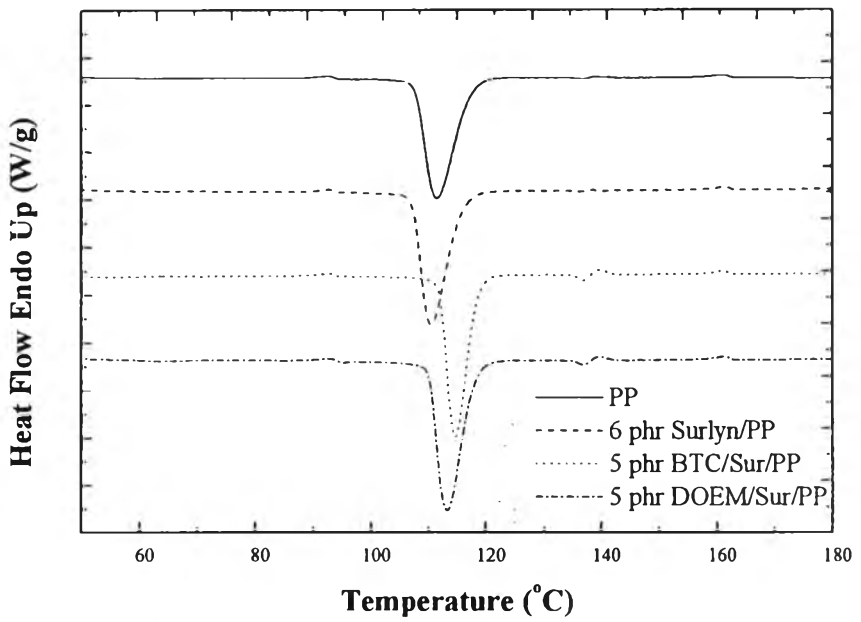

Figure 4.9 Effect of type of organoclay on the crystallization temperature (T_c) of the fibers

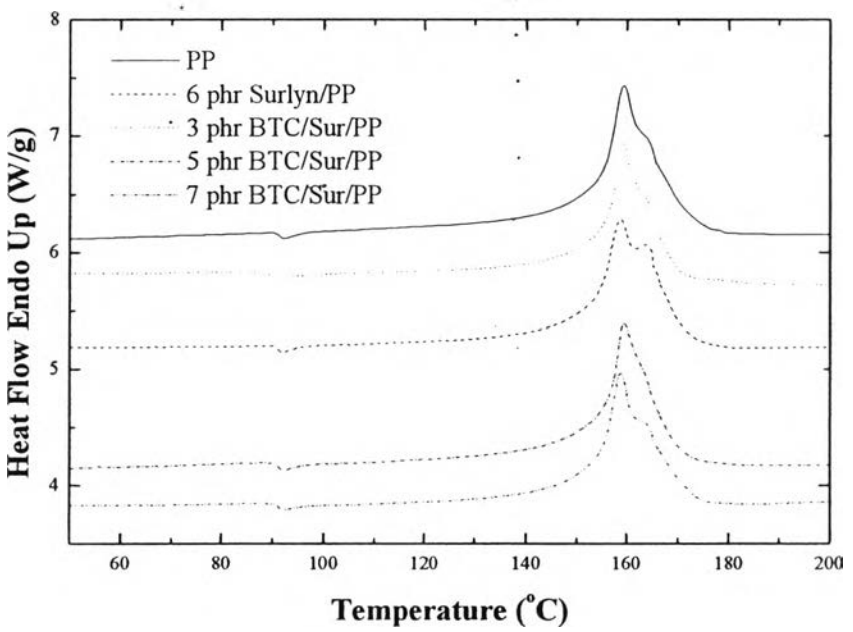

Figure 4.10 Effect of amount of organoclay on the melting temperature (T_m) of the fibers

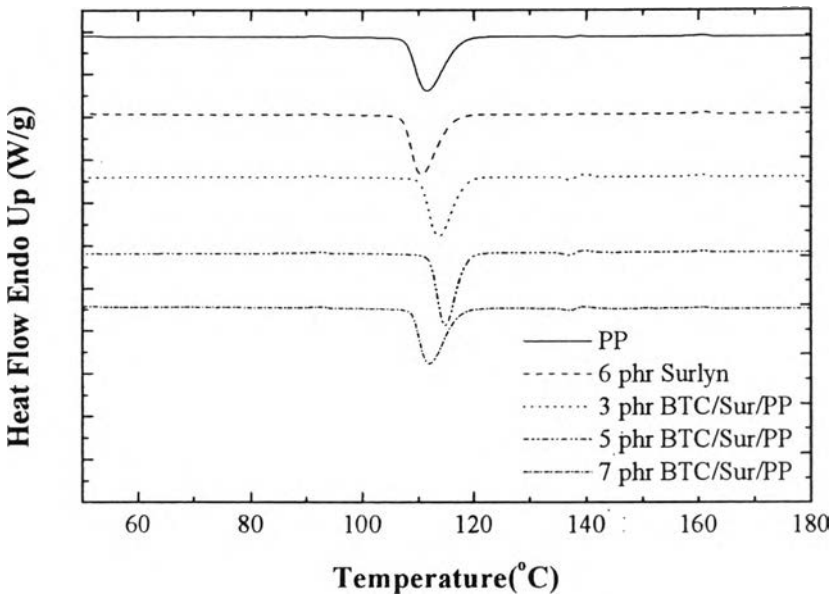

Figure 4.11 Effect of amount of organoclay on the crystallization temperature (T_c) of the fibers

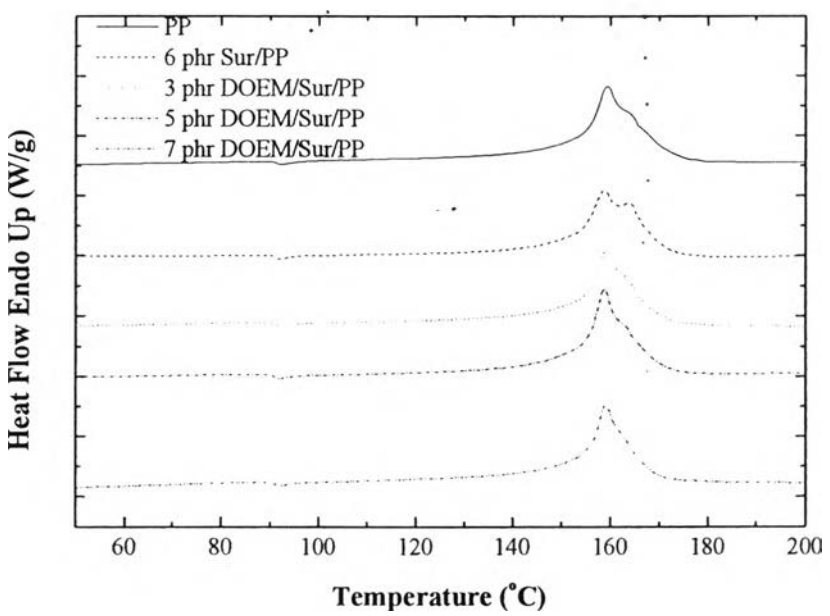

Figure 4.12 Effect of amount of DOEM-organoclay on the melting temperature (T_m) of the fibers

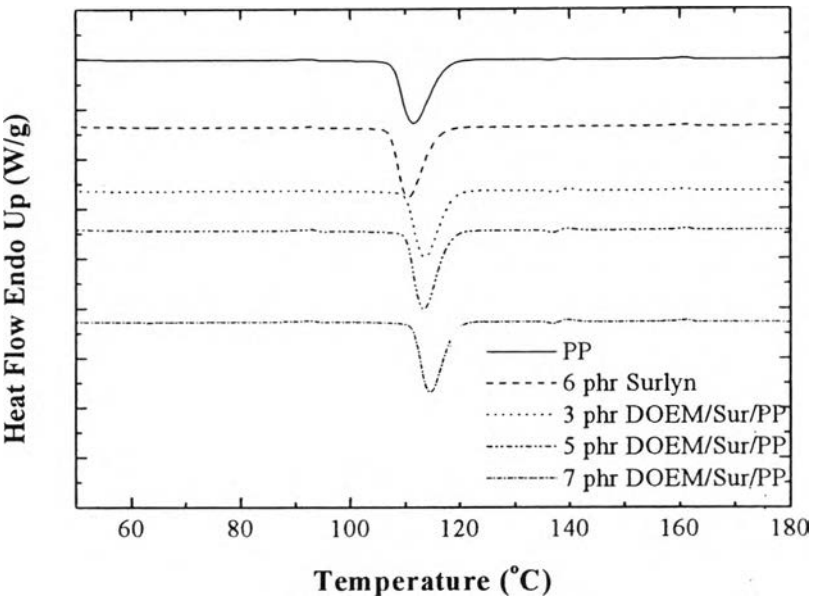

Figure 4.13 Effect of amount of organoclay on the crystallization temperature (T_c) of the fibers

Table 4.3 Effect of compatibilizers on thermal and crystal behavior of fibers

Samples	T_c (Peak) (°C)	T_c (Onset) (°C)	T_m (Peak) (°C)	T_m (Onset) (°C)	ΔH_m (J/g)	% Crystallinity
PP	111.47	117.39	159.37	154.03	70.35	33.66
6 phr Surlyn/PP	110.47	114.47	158.7	152.96	63.84	30.54
15 phr PP-g-MAH/PP	116.47	117.13	159.53	155.10	66.69	31.91
5 phr BTC/Surlyn/PP	114.80	118.45	159.53	155.54	72.48	34.68
5 phr BTC/PP-g-MAH/PP	117.13	120.59	159.53	155.24	78.98	37.79

Table 4.4 Effect of surfactant on thermal and crystal behavior of fibers

Samples	T_c (Peak) (°C)	T_c (Onset) (°C)	T_m (Peak) (°C)	T_m (Onset) (°C)	ΔH_m (J/g)	% Crystallinity
PP	111.47	117.39	159.37	154.03	70.35	33.66
6 phr Surlyn/PP	110.47	114.47	158.7	152.96	63.84	30.54
5 phr BTC/Surlyn/PP	114.80	118.45	159.53	155.54	72.48	34.68
5 phr DOEM/Surlyn/PP	113.30	118.03	158.7	154.21	72.27	34.58

Table 4.5 Effect of amount of organoclay on thermal and crystal behavior of fibers

Samples	T_c (Peak) (°C)	T_c (Onset) (°C)	T_m (Peak) (°C)	T_m (Onset) (°C)	ΔH_m (J/g)	% Crystallinity
PP	111.47	117.39	159.37	154.03	70.35	33.66
6 phr Surlyn/PP	110.47	114.47	158.7	152.96	63.84	30.54
3 phr BTC/Surlyn/PP	113.63	118.26	159.2	155.07	71.60	34.26
5 phr BTC/Surlyn/PP	114.8	118.45	159.53	155.54	72.48	34.68
7 phr BTC/Surlyn/PP	111.97	117.12	158.87	153.90	70.09	33.54
3 phr DOEM/Surlyn/PP	113.47	118.47	159.2	154.70	74.78	35.78
5 phr DOEM/Surlyn/PP	113.30	118.03	158.7	154.21	72.27	34.58
7 phr DOEM/Surlyn/PP	114.47	119.02	159.03	154.78	73.89	35.35

Table 4.6 Effect of draw ratio on thermal and crystal behavior of fibers

Samples	Draw ratio	T_c (Peak) (°C)	T_c (Onset) (°C)	T_m (Peak) (°C)	T_m (Onset) (°C)	ΔH_m (J/g)	% Crystallinity
PP	15.3	109.97	115.55	164.33	157.12	64.45	30.84
	26.5	111.47	117.39	164.33	157.19	66.02	31.59
	35.6	110.30	115.85	164.67	157.95	79.53	38.05
	47.6	110.63	116.24	164.50	158.42	80.18	38.36
5 phr BTC/Sur/PP	15.3	114.80	118.83	164.50	156.96	63.98	30.61
	26.5	114.63	118.58	164.54	156.94	64.94	31.07
	35.6	114.97	118.81	164.75	159.43	66.20	31.68
	47.6	114.63	118.74	166.00	158.68	67.82	32.45
5 phr DOEM/Sur/PP	15.3	113.30	118.15	165.33	157.27	66.92	32.02
	26.5	113.30	118.03	164.83	157.55	74.78	34.31
	35.6	113.13	117.89	165.00	157.86	67.82	34.52
	47.6	113.30	118.07	165.17	158.72	73.89	36.46

4.4.3 Orientation of Organoclay-PP nanocomposite Fiber

The orientation of the fibers was studied using infrared spectroscopy collected from polarization radiation parallel and perpendicular to the fiber axis. In the typical IR spectrums, the absorption band at 841 cm^{-1} is attributed to crystalline phase being assigned to the CH_2 rocking deformation mode. For the absorption band at 1256 cm^{-1}, this band has been attributed to both crystalline and amorphous phase and assigned to the twisting of the CH_2 group coupled with the axial and equatorial bending CH modes. The infrared dichroism of this band was taken to correlate with

some average orientation function [20]. The value of dichroic ratio, crystalline (F_{841}) and average orientation (F_{1256}), and angle of orientation were shown in the table 4.7. Fibers extruded with higher speed gave the lower angle of orientation implied that the fibers were oriented more parallel to the draw direction. Draw ratio gave more significant effect to unmodified-PP fibers than the organoclay PP fibers. Clay molecules can interrupt the orientation of the polymer molecules. The orientation angle reduced abruptly from draw ratio 15.3 to 26.5 x1000 and became rather steady with increasing draw ratio. For DOEM/PP fiber, the orientation angle increased at high draw ratio, probably due to bending mode of CH arranged away from the draw axis to reduce steric effect when the chain was drawn.

Table 4.7 Orientation of the fibers

Samples	Draw ratio (X1000)	Dichroic ratio		Orientation function		Angle of orientation	
		D_{841}	D_{1256}	F_{841}	F_{1256}	θ_{841}	θ_{1256}
PP	15.3	0.911	0.916	-0.038	-0.051	56.28	56.84
	26.5	0.998	1.020	-0.001	0.012	54.76	54.25
	36.6	1.076	1.141	0.030	0.080	53.51	51.54
	47.6	1.201	1.470	0.077	0.242	51.66	45.29
5 phr BTC/Sur/PP	15.3	0.822	0.806	-0.078	-0.124	57.96	59.95
	26.5	1.088	1.077	0.035	0.045	53.32	52.94
	36.6	0.941	1.069	-0.025	0.040	55.74	53.12
	47.6	1.212	1.094	0.081	0.055	51.51	52.55
5 phr DOEM/Sur/PP	15.3	0.844	1.012	-0.067	0.007	57.52	54.44
	26.5	1.019	0.839	0.008	-0.102	54.42	58.98
	36.6	0.974	0.926	-0.011	-0.045	55.17	56.58
	47.6	1.063	0.900	0.025	-0.062	53.72	57.29

* φ_{841}= 14.3° and φ_{1256} = 32.9 °

4.4.4 Morphology of Organoclay-PP Fiber

Morphology of the modified fibers from SEM shown that there was poor interaction between PP and organoclay. The lateral size of clay was about 1-5 μm. It can be observed that the fibers consisted of both composite intercalation and conventional composites. From SEM image of BTC/PP fibers, organoclay molecules were in the polymer matrix. EDX analysis was used to indicate the element composition in the organoclay/PP nanocomposite fibers. According to the EDX

results (Fig. 4.14), they revealed the distribution of Si. If the amount of organoclay increases, the SEM-EDX images exhibit large cluster of clay particles disperses in the PP matrix. Moreover, the clay particles in 3 phr clay/polypropylene nanocomposites were finer than those in 5 and 7 phr organoclay/PP suggesting better cracking of clay particles by shearing in extrusion.

Surface morphology of nanocomposite fibers were observed using tapping mode of Scanning Probe Microscope (SPM). The SPM micrograph shown that clay molecules were presented on both BTC and DOEM modified PP fibers presented clay molecule on the fiber surface. Fig 4.15 and table 4.8 indicate that unmodified–PP fiber was a smooth surface, whereas organoclay/PP nanocomposite fibers shown a rougher surface. Comparing between BTC/PP and DOEM/Surlyn/PP fibers, BTC/Surlyn/PP fiber has higher mean roughness value than that of DOEM/PP fiber. In addition, mean roughness values increased as draw ratio increased.

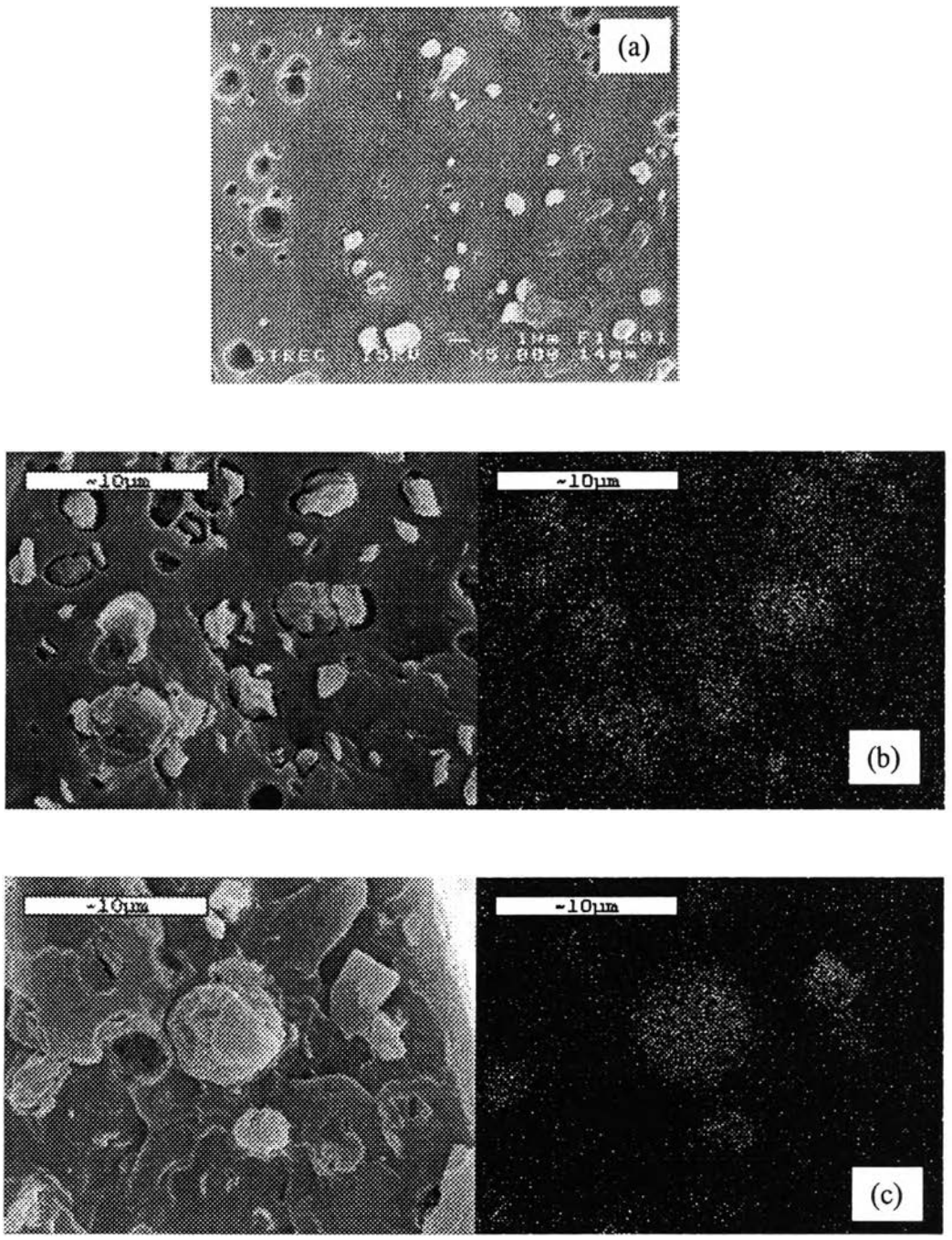

Figure 4.14 SEM and SEM-EDX images of fiber cross-section (a) 3 phr BTC/Sur/PP (b) 5 phr BTC/Sur/PP (c) 7 phr BTC/Sur/PP

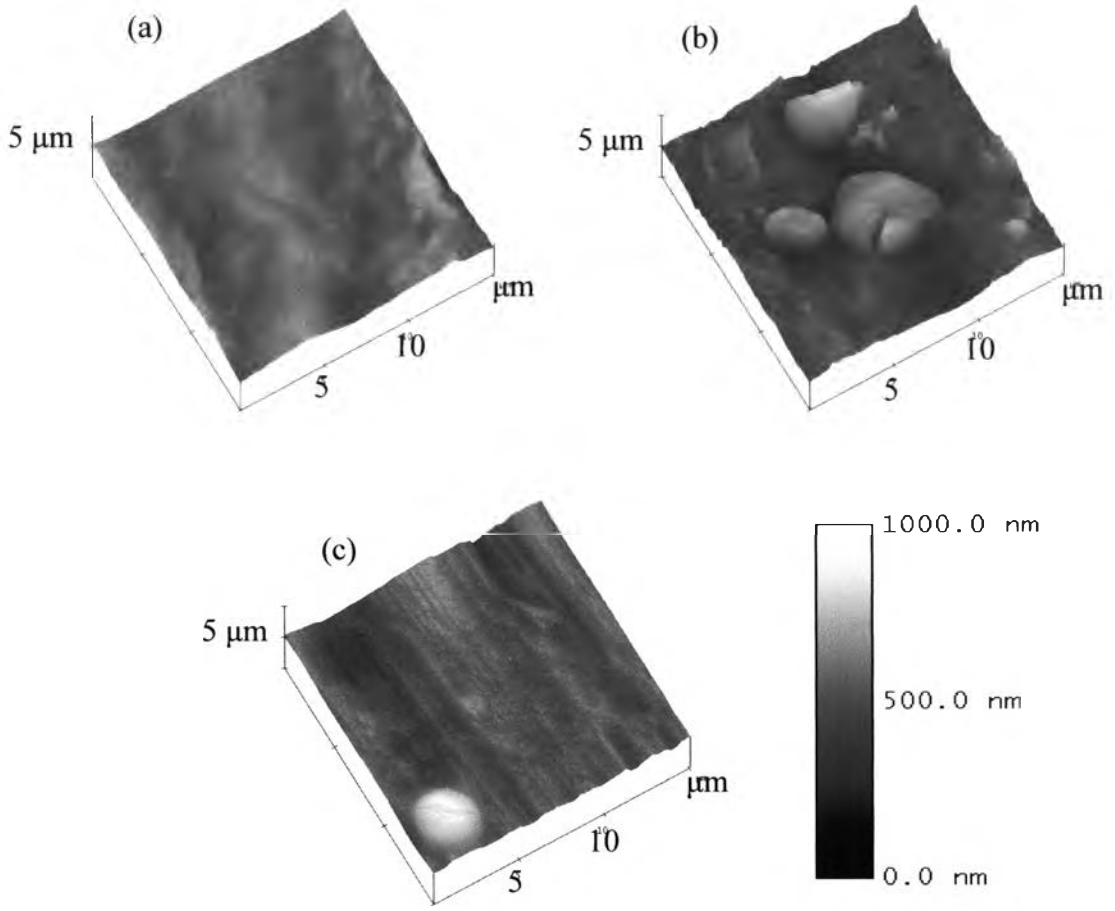

Figure 4.15 SPM images of fiber surface (a) PP fiber (b) 5 phr BTC/Sur/PP fiber (c) 5 phr DOEM/Sur/PP fiber

Table 4.8 Mean roughness values of PP and organoclay-PP nanocomposite fibers

Samples	Draw ratio (x1000)	Mean roughness (nm)
PP	26.5	39.947
5 phr BTC/sur/PP	15.3	86.288
5 phr BTC/sur/PP	26.5	94.757
5 phr BTC/sur/PP	35.6	98.752
5 phr BTC/sur/PP	47.6	123.77
5 phr DOEM/sur/PP	26.5	53.051

4.4.5 Mechanical Properties

One of the advantages of adding organoclay into polymer is to improve the mechanical properties of the material. From Fig. 4.16, fiber with 5 phr BTC shows the higher stress at break than the unmodified PP fiber. However, the organoclay–modified PP fibers give an increase of Young's Modulus when compare to the unmodified PP fiber (Fig. 4.17). BTC–organoclay/PP fibers has lower %strain at break than that of the neat PP fiber and these values decreased as amount of BTC–organoclay increased, this is because clay molecules allow cracking initiation and propagation (Fig. 4.18). Whereas, DOEM-organoclay/PP fibers gives an increasing of %strain at break when compare to the unmodified PP fiber because surface of these fibers contain less grooves and flaws than BTC/PP fibers so there are less possibility of cracking initiation and propagation. Draw ratio also play an important role on the mechanical properties of the fibers. From Fig. 4.19-4.21, the stress and Young's Modulus of organoclay–PP fiber were increased because of the higher crystallization and orientation in the draw direction resulting in the higher intermolecular force between polymer chains. Whereas, the % elongation of the fiber is decreased as the draw ratio increase because the smaller diameter of fiber can be extended to the length less than the bigger one.

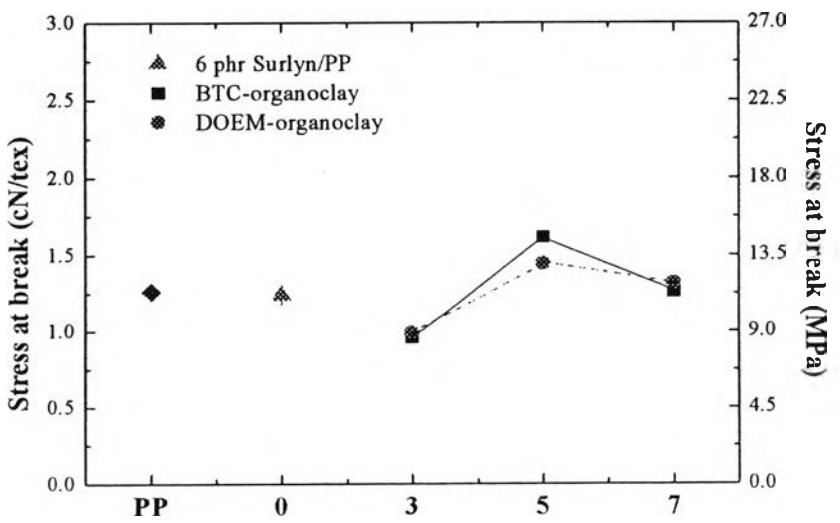

Figure 4.16 Stress at break of PP and organoclay/PP nanocomposite fibers

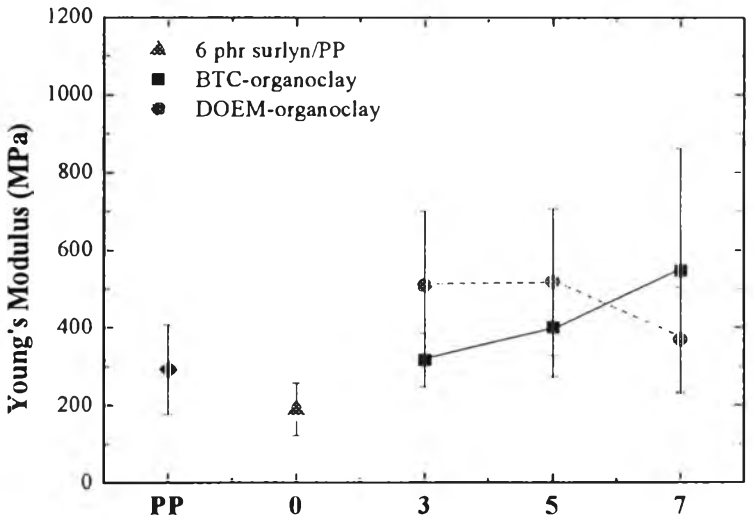

Figure 4.17 Young's Modulus of PP and organoclay/PP nanocomposite fibers

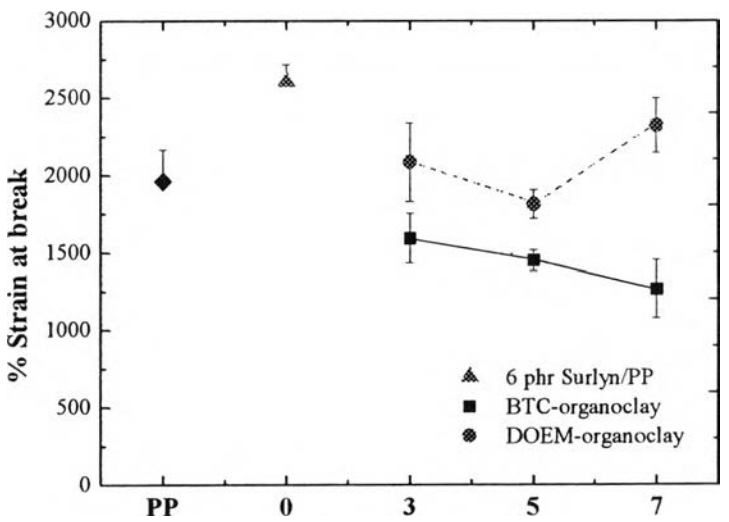

Figure 4.18 % Strain at break of PP and organoclay/PP nanocomposite fibers

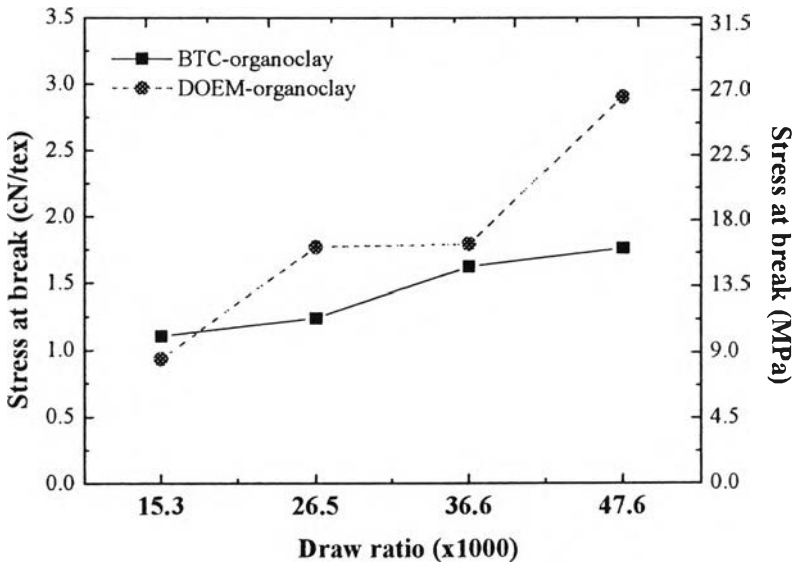

Figure 4.19 Stress at break of BTC and DOEM organoclay/PP fiber with various draw ratio

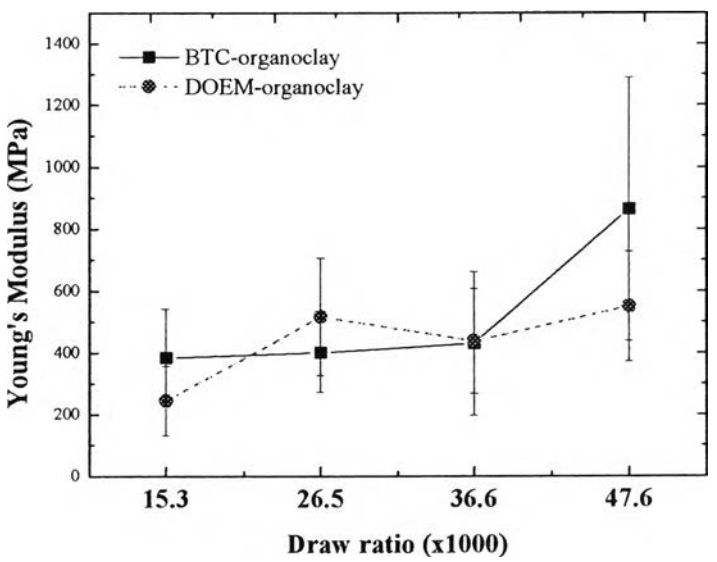

Figure 4.20 Young's Modulus of BTC and DOEM organoclay/PP fiber with various draw ratio

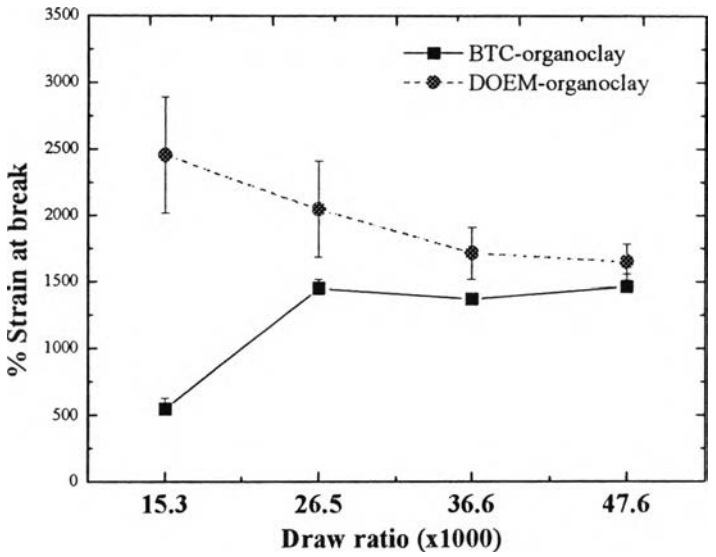

Figure 4.21 % Strain at break of BTC and DOEM organoclay/PP fiber with various draw ratio

4.4.6 *Dyeing properties*

Dyeing properties of fiber can be studied by measuring the different absorbance of dye solution before and after dyeing process. The absorbance can then be converted to % dye exhaustion which is the amount of dye absorbed by the fiber. In addition, the color intensity of the dyed fibers were measured by flectance mode of uv-visible spectrophotometry and the CIE colorimetry.

From the color build up curve (Fig. 4.22), no significant different in the color of the fiber when dyed at dye concentration is observed. Therefore, 2% dye concentration was selected as dye concentration used in the study.

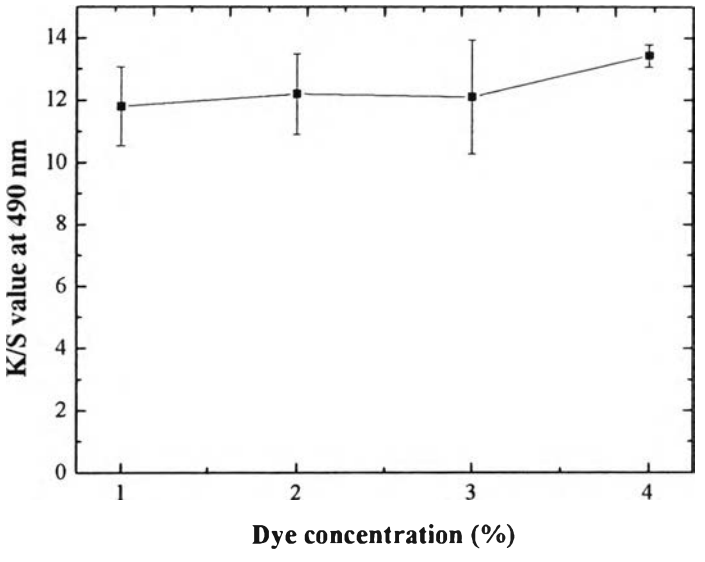

Figure 4.22 Color build up curve of 5 phr BTC/Surlyn/PP fibers dyed with disperse dye

Compatibilizers were used in the organoclay to help polypropylene and organoclay more compatible. In this work, Surlyn and PP-g-MAH were used to improve compatibility between clay and PP. Fiber with surlyn as a compatibilizer were found to give better dyeability than that of PP-g-MAH (Fig. 4.23 – 4.24). This result was related to the result of orientation of the fiber (mention in the earlier section) in PP-g-MAH led to more orientation of the fiber molecules so it was more difficult for dye molecule to penetrate inside the fiber. This result was confirmed by CIE colorimetry, the fiber with Surlyn as a compatibilizer dyed with acid dye gave the dE* (with PP fiber taken as the standard) higher than that of PP-g-MAH, this indicated that the fiber was dyed to the shade when compared to standard PP more than fiber with PP-g-MAH as a compatibilizer (Table 4.9). In addition, it had the highest da* which is the indicator value for the redness-greeness of the sample, so the results indicated that the fiber with Surlyn as a compatibilizer were more red than the standard and deeper in the red shade than that with PP-g-MAH as compatibilizer when compare with the same standard. On the other hand, fiber with PP-g-MAH as a compatibilizer which dyed with disperse dye show much improve in dE* value. So

the disperse dye can be interacted with this fiber more efficient than other types pf dye.

Surfactant that was used to modified nanoclay also played an important role in dyeing properties of the fibers. The result from K/S values indicated that effect of BTC–organoclay to improve the dye absorption of the fiber was better than that of DOEM–organoclay (Fig. 4.25 – 4.26). For basic and direct dye, both BTC and DOEM organoclay show the color intensity close to that of the unmodified PP fiber. Similary, BTC–organoclay fiber show dE* and da* higher than DOEM/PP fiber in case of dyeing with acid, direct, and disperse dyes (Table 4.10). However, the optical microscope image of fiber dyed with direct dye showed lighter shade and poor dyeability (Fig 4.33). The results suggested that effect of aromatic interaction between BTC–organoclay molecules and the dye molecules is more significant than polar-polar interaction between DOEM–organoclay molecules and the dyes. And from the result of SEM and SPM images shown that BTC–organoclay/PP nanocomposite fiber has rough surface and this rough surface will provide more channel for dye molecules for enter inside the fiber. When compare the dye uptake and K/S value (color intensity) of fiber dyed with the different 4 types of dye (Fig. 4.23 – 4.26), high values were observed in the organoclay/PP fibers dyed with disperse and acid dyes, but relatively low sorption of the basic and direct dyes. Although, the direct dye gave the dye uptake of fiber higher than the other types of dye, the color intensity of the fibers was low. This result suggested that direct dye cannot be absorbed strongly inside the fibers and can be removed easily by washing with water. The images from the optical microscope shown that the disperse dye molecule can penetrate into the fiber cross section better than other types of dyes (Fig. 4.39). Although the organoclay/PP fiber dyed with acid dye shown the redder shade than the unmodified PP fiber and better than basic and direct dyes (Fig. 4.31, 4.33, and 4.35), the cross section images shown the light color at the center of the fibers which implied that dye molecules are only absorbed on the fiber surface and only small amount of dye molecules were penetrated into the fiber (Fig. 4.32). The results suggested that the major forces for dye absorption are Van der Waals force and hydrophobic interaction from disperse dye. Ionic force also played an important role which can be seen from anion of acid dye that can interact with cation of

surfactant modified clay. In the case of basic dye, there was repulsive force between cations of dye and cationic surfactant.

Effect from amount of organoclay on dyeability of organoclay/PP fiber was also studied. The disperse and acid dyes were selected for this experiment due to the high absorption of the two types of dye on the fiber. Fig. 4.27 shown that color intensity of organoclay/PP fiber dyed with disperse dye is gradually increase as the amount of organoclay increase. However, for acid dye, the color intensity was obviously increased at 5 and 7 phr for BTC–organoclay and DOEM-organoclay respectively (Fig. 4.28). This result showed the similar trend to the CIE parameter in the case of disperse dye in that the dE* and da* gradually increase as the clay content increase (Table 4.11). For the acid dye, BTC organoclay shown an increasing of dE* at higher clay content but dropped a little at 7 phr BTC/Surlyn/PP (Table 4.11).

Fiber can be extruded with different draw ratio to produce fiber with different diameter. In addition, an increasing draw ratio can also affect the orientation, crystallinity, and surface roughness of the fiber. However, these three parameters gave the different effect to the dyeability of the fiber. When crystallization and orientation were increased, the higher order of polymer chains was obtained so it is become more difficult for dye molecules to penetrate into the fibers. On the other hand, the greater surface roughness resulted in the flaws and grooves presented at the surface of the fiber and provide more channel for the penetration of dye molecules into the fiber. Fig 4.29 and 4.30 showed that the dye absorption of the fibers tend to be reduced as the draw ratio increase. It was suggested that the effect from crystallization and orientation was more significant than effect from surface roughness.

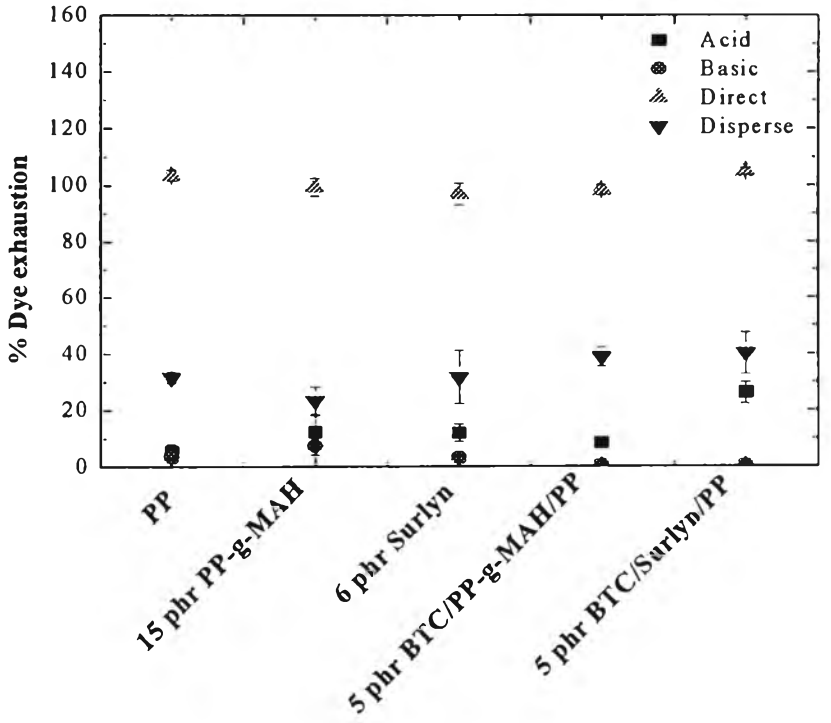

Figure 4.23 % Dye exhaustion of PP and modified PP fiber with various compatibilizers

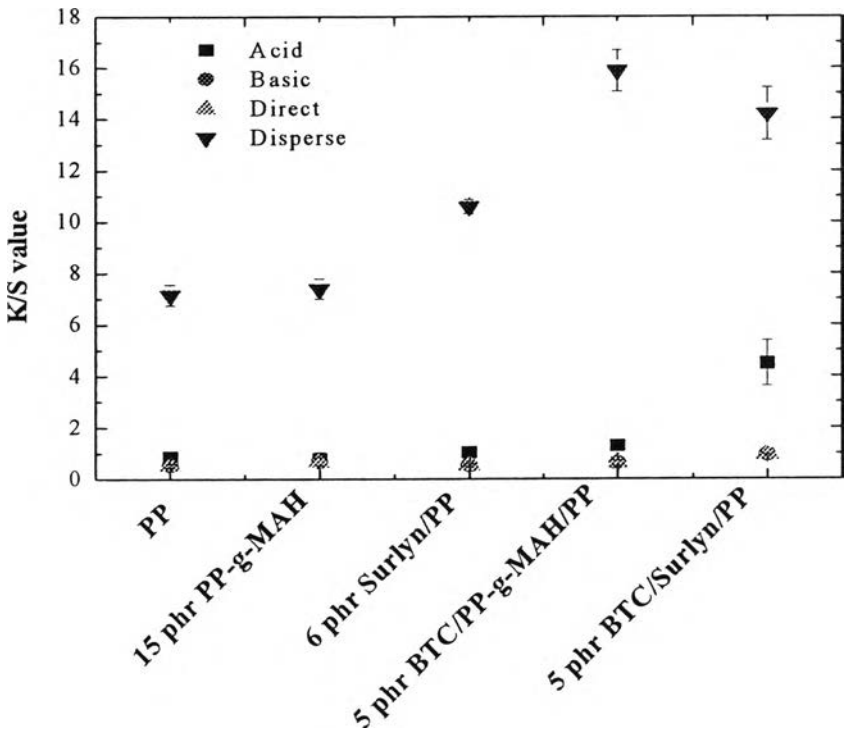

Figure 4.24 K/S values of PP and modified PP fiber with various compatibilizers

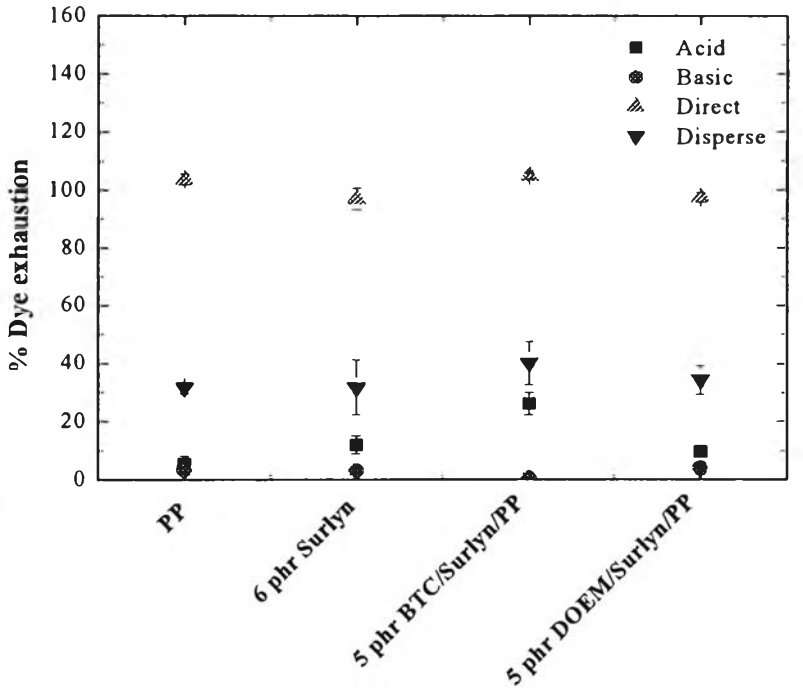

Figure 4.25 % Dye exhaustion of PP and modified PP fiber with various organoclays

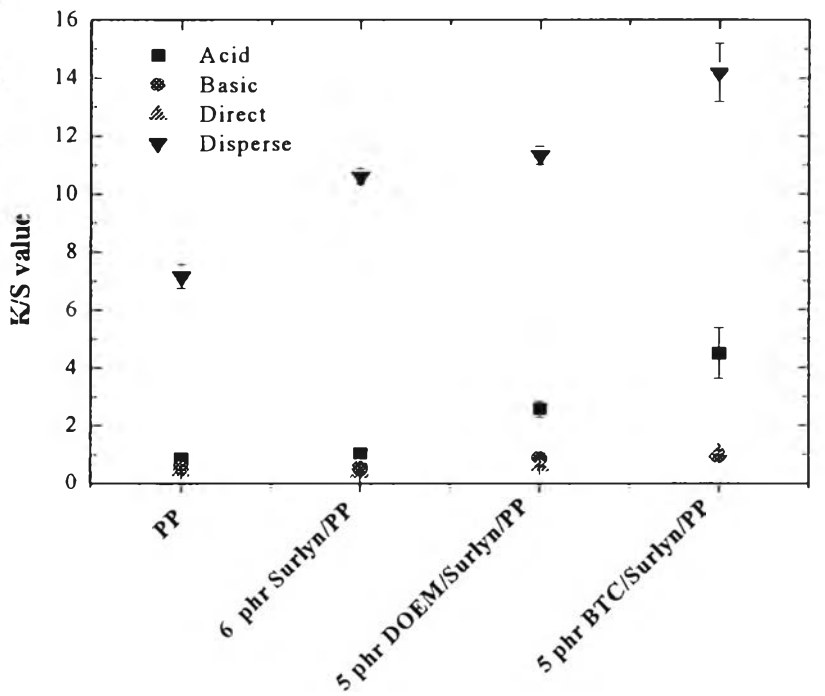

Figure 4.26 K/S values of PP and modified PP fiber with various organoclays and dyed with 4 different types of dye

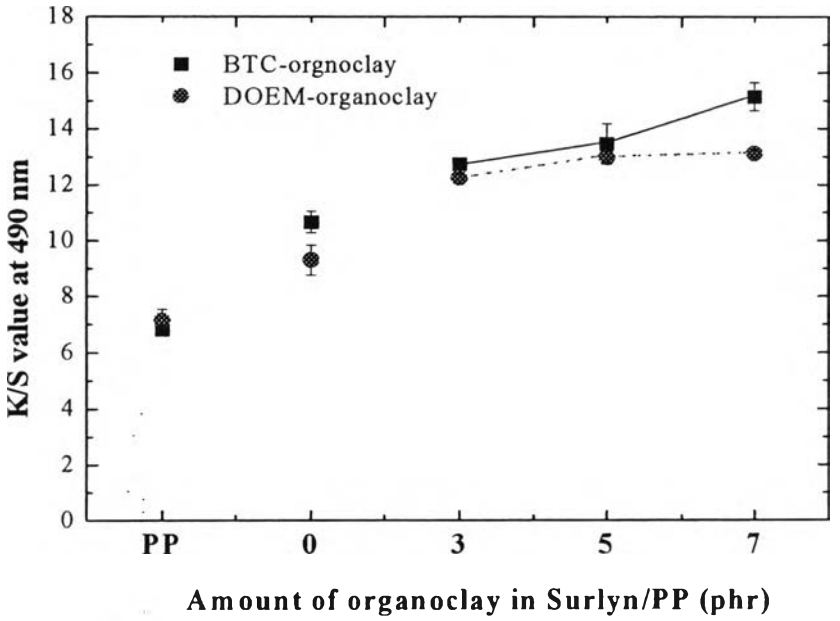

Figure 4.27 K/S values of disperse dyed PP fibers modified with various amount of organoclay

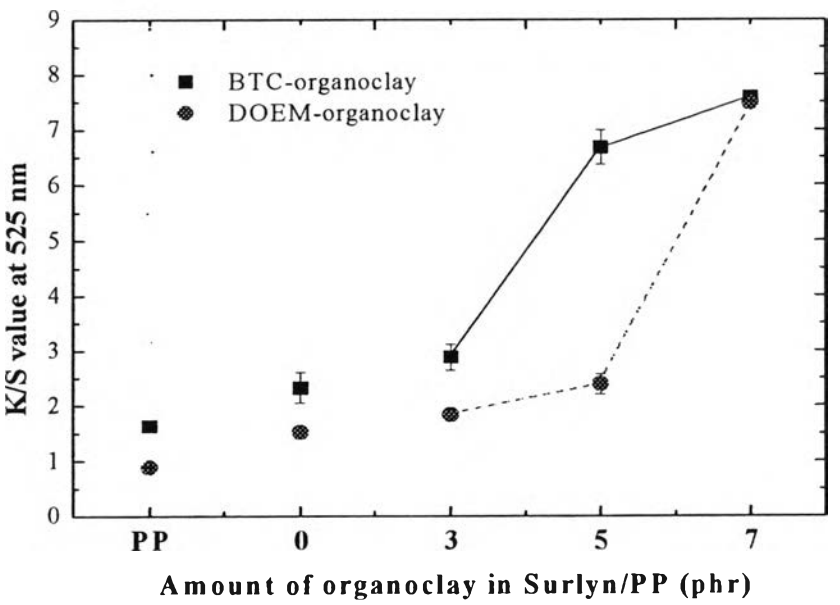

Figure 4.28 K/S values of acid dyed PP fibers modified with various amount of organoclay

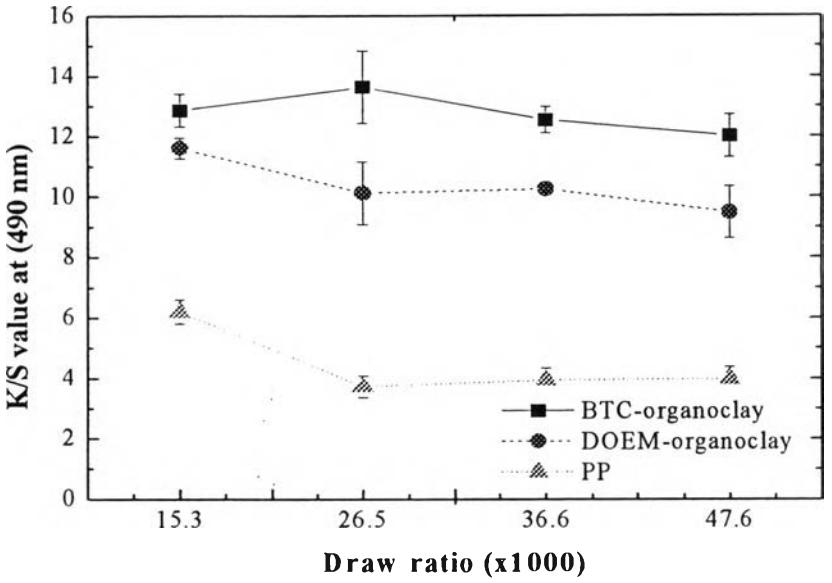

Figure 4.29 K/S values of disperse dyed fibers extruded with different draw ratio

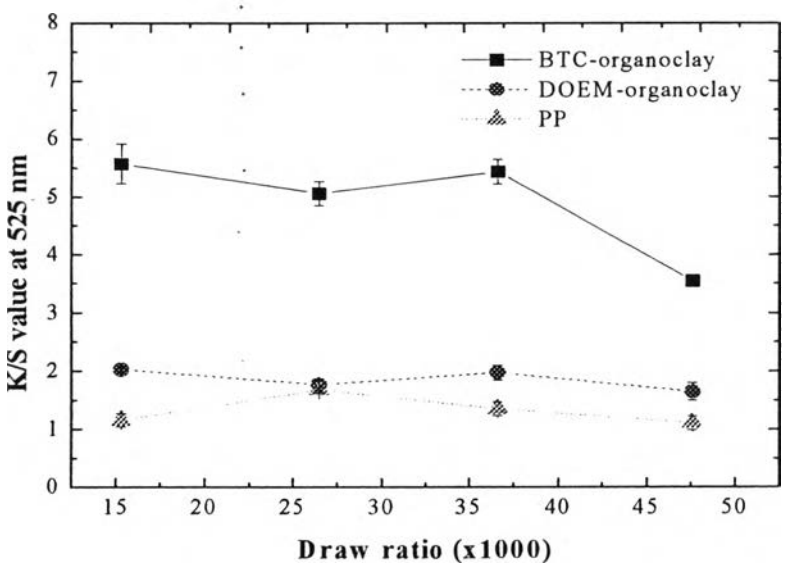

Figure 4.30 K/S values of acid dyed fibers extruded with different draw ratio

Table 4.9 Color intensity reading (CIE parameter) of dyed fibers with different types of dye and compatibilizers.

Dyes	Sample	L*	a*	b*	dL*	da*	db*	dE*
Acid	PP	49.86	13.33	7.72				
	6 phr Surlyn	46.57	12.50	3.22	-3.30	-0.84	-4.51	5.65
	15 phr PP-g-MAH	50.65	13.89	6.31	0.79	0.55	-1.41	1.71
	5 phr BTC/Surlyn/PP	43.52	32.33	7.84	-6.34	18.99	0.11	20.02
	5 phr BTC/PP-g-MAH/PP	49.03	17.31	7.02	-0.83	3.98	-0.70	4.13
Basic	PP	51.81	5.47	7.36				
	6 phr Surlyn	50.09	6.58	5.49	-1.72	1.11	-1.87	2.77
	15 phr PP-g-MAH	51.68	8.46	6.29	-0.12	2.99	-1.07	3.18
	5 phr BTC/Surlyn/PP	52.67	9.37	8.77	0.87	3.90	1.41	4.24
	5 phr BTC/PP-g-MAH/PP	53.31	6.47	9.78	1.51	1.01	2.42	3.02
Direct	PP	51.92	7.23	3.73				
	6 phr Surlyn	59.17	7.11	6.84	7.25	-0.11	3.11	7.89
	15 phr PP-g-MAH	47.97	6.08	4.31	-3.95	-1.15	0.58	4.16
	5 phr BTC/Surlyn/PP	57.33	20.03	9.33	5.41	12.80	5.60	14.98
	5 phr BTC/PP-g-MAH/PP	54.49	7.01	9.78	2.57	-0.22	6.04	6.57
Disperse	PP	34.97	25.63	20.09				
	6 phr Surlyn	30.50	28.49	18.45	-4.47	2.86	-1.64	5.56
	15 phr PP-g-MAH	36.39	30.59	22.32	1.42	4.96	2.23	5.62
	5 phr BTC/Surlyn/PP	23.13	28.28	11.26	-11.84	2.65	-8.83	15.00
	5 phr BTC/PP-g-MAH/PP	15.96	20.91	6.43	-19.01	-4.72	-13.66	23.88

Table 4.10 Color intensity reading (CIE parameter) of dyed fibers with different types of dye and surfactants used to modified clay.

Dyes	Samples	L*	a*	b*	dL*	da*	db*	dE*
Acid	PP	49.86	13.33	7.72				
	6 phr Surlyn	46.57	12.50	3.22	-3.30	-0.84	-4.51	5.65
	5 phr BTC/Surlyn/PP	43.52	32.33	7.84	-6.34	18.99	0.11	20.02
	5 phr DOEM/Surlyn/PP	47.24	29.81	8.13	-2.62	16.48	0.40	16.69
Basic	PP	51.81	5.47	7.36				
	6 phr Surlyn	50.09	6.58	5.49	-1.72	1.11	-1.87	2.77
	5 phr BTC/Surlyn/PP	52.67	9.37	8.77	0.87	3.90	1.41	4.24
	5 phr DOEM/Surlyn/PP	52.90	10.21	7.13	1.10	4.75	-0.22	4.88
Direct	PP	51.92	7.23	3.73				
	6 phr Surlyn	59.17	7.11	6.84	7.25	-0.11	3.11	7.89
	5 phr BTC/Surlyn/PP	57.33	20.03	9.33	5.41	12.80	5.60	14.98
	5 phr DOEM/Surlyn/PP	59.29	11.14	9.28	7.37	3.92	5.54	10.02
Disperse	PP	34.97	25.63	20.09				
	6 phr Surlyn	30.50	28.49	18.45	-4.47	2.86	-1.64	5.56
	5 phr BTC/Surlyn/PP	23.13	28.28	11.26	-11.84	2.65	-8.83	15.00
	5 phr DOEM/Surlyn/PP	27.54	30.01	19.12	-7.43	4.38	-0.97	8.67

Table 4.11 Color intensity reading (CIE parameter) of dyed fibers with various clay content

Amount of organoclay in Surlyn/PP (phr)	L*	a*	b*	dL*	da*	db*	dE*
Disperse dye							
PP	48.28	18.29	10.63				
0	48.37	22.68	10.84	0.09	4.39	0.21	4.39
3	47.45	30.89	7.98	-0.84	12.60	-2.65	12.90
5	37.88	36.61	11.32	-10.40	18.32	0.68	21.08
7	40.03	36.00	10.99	-8.26	17.71	0.36	19.54
Acid dye							
PP	49.86	13.33	7.72				
0	51.86	19.27	8.37	2.00	5.93	0.64	6.29
3	52.76	26.18	10.41	2.90	12.84	2.68	13.43
5	46.49	23.60	7.06	-3.37	10.27	-0.67	10.83
7	36.73	36.07	15.63	-13.13	22.74	7.91	27.42

The surface and color of the fibers can be observed by optical microscope (Fig. 4.30 – 4.35). Images of fiber show that both BTC and DOEM organoclay/PP fibers have opaque and rough surface, on the other hand, unmodified fiber show smoother surface. And the images can show the dye dispersion not only on the fiber surface but also inside the fibers. From figure 4.30, BTC/PP fiber dyed with acid dye show small red dot, this probably due to the attraction of dye molecule on the larger size of organoclay in PP matrix. The DOEM/PP fiber has lighter color than BTC/PP fiber (Fig. 4.30(b) and (c). For basic and direct dye, the color of the modified fiber cannot be observed by optical microscope (Fig. 4.31-4.32). From figure 4.33, the image of PP fiber indicated that PP can be slightly dyed with disperse dye. In addition, organoclay/PP fiber shows much improvement of the dyeability of the fiber. BTC organoclay result in more color concentration than DOEM organoclay. 5 phr BTC/PP-g-MAH/PP fiber has the highest color intensity, probable due to BTC/PP-g-MAH/PP fiber has larger size of clay cluster on the fiber surface than BTC/Surlyn/PP fiber. Figure 4.34 can be obviously seen that fiber extruded with draw ratio 47.6x1000 has the lightest color than the others which is related to the result from K/S value from uv-visible spectrophotometry.

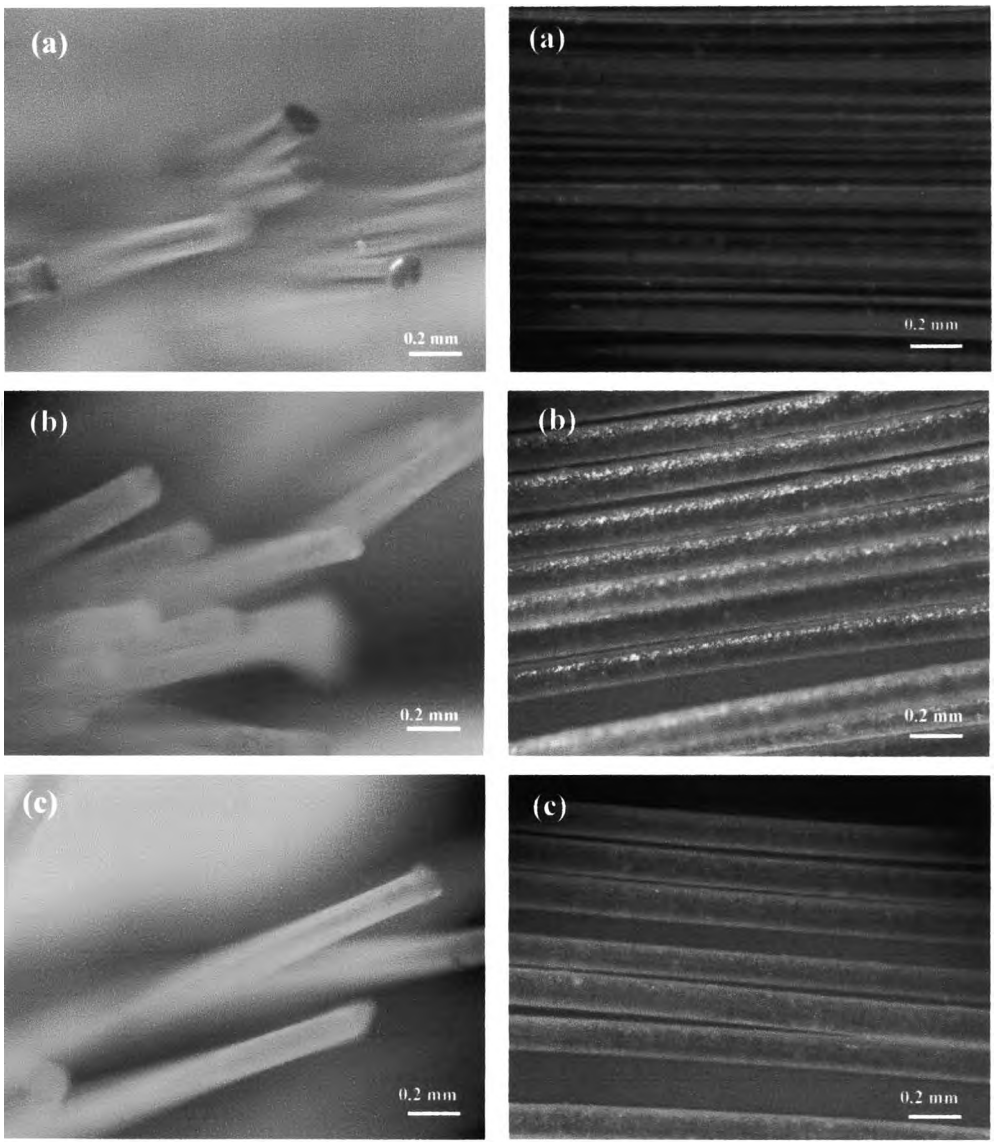

Figure 4.31 Images (120x) of fibers dyed with acid dye (a) PP (b) 5 phr BTC/Surlyn/PP (c) 5 phr DOEM/Surlyn/PP

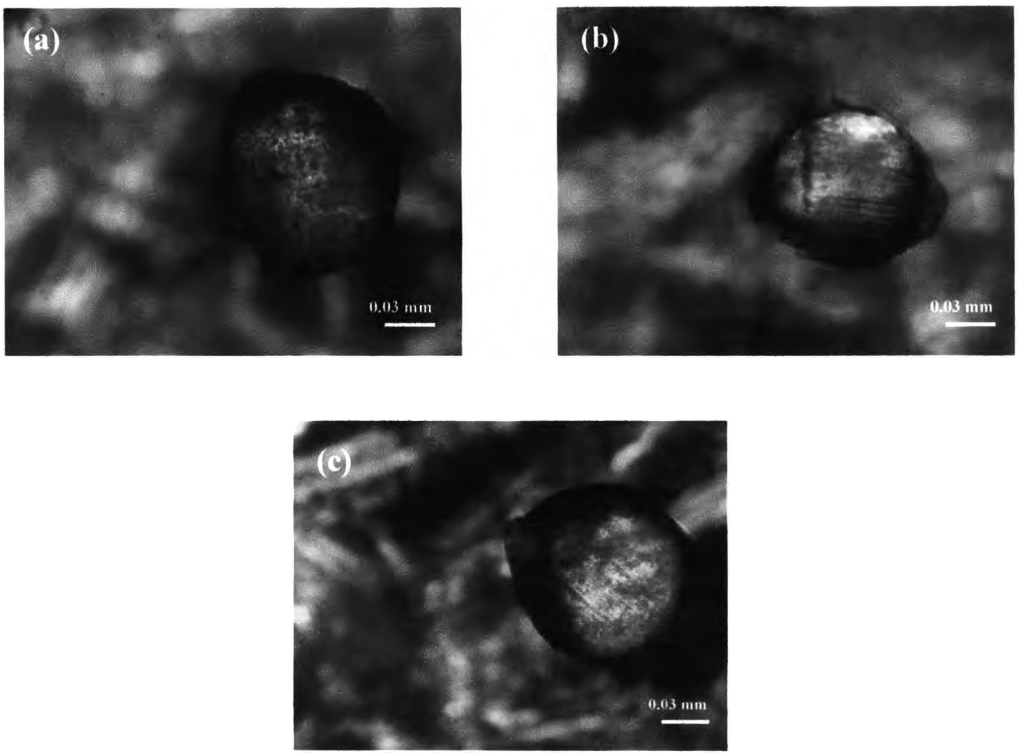

Figure 4.32 Images (600x) of fiber cross-section dyed with acid dye (a) PP (b) 5 phr BTC/Surlyn/PP (c) 5 phr DOEM/Surlyn/PP

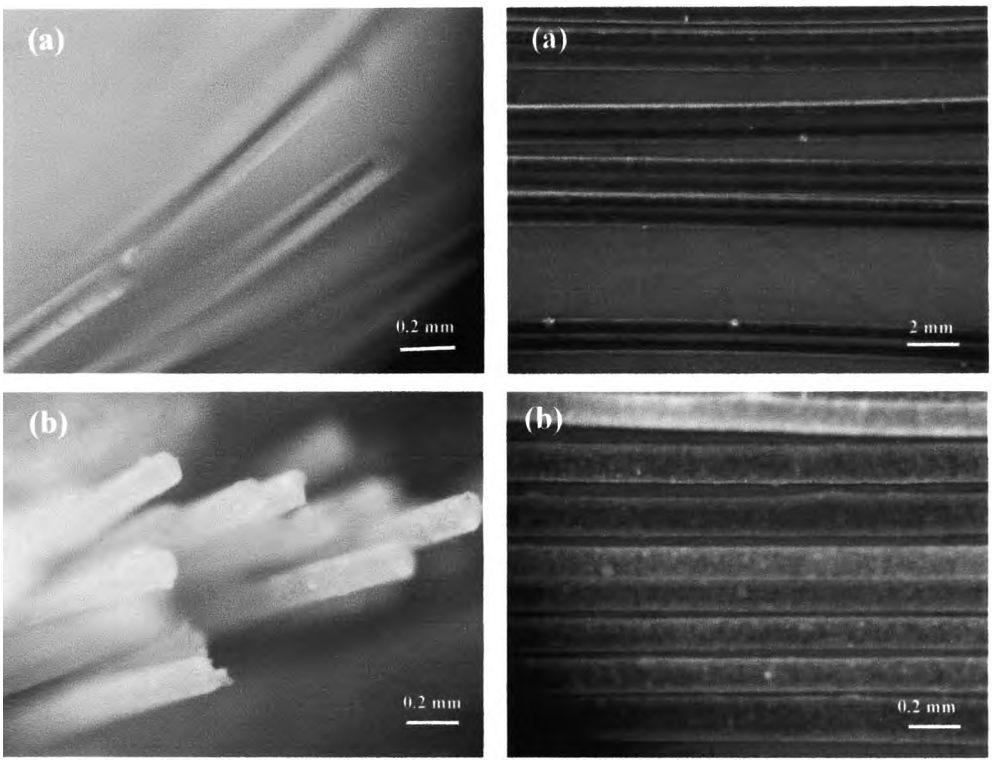

Figure 4.33 Images (120x) of fibers dyed with basic dye (a) PP (b) 5 phr BTC/Surlyn/PP

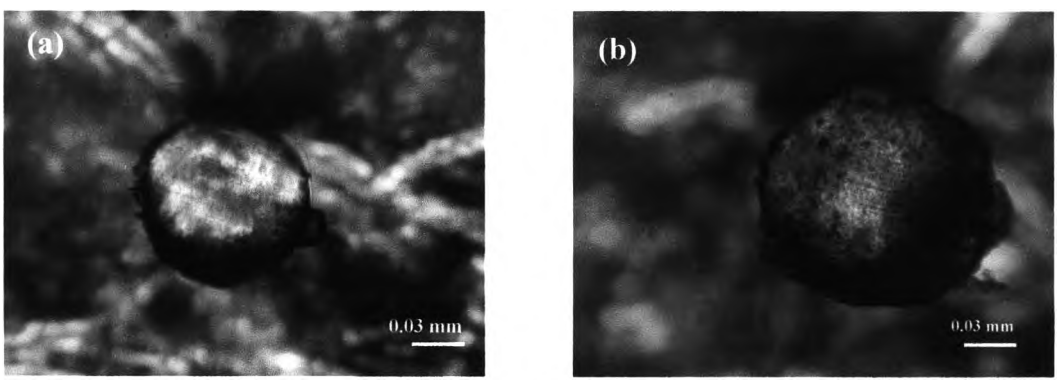

Figure 4.34 Images (600x) of fiber cross-section dyed with basic dye (a) PP (b) 5 phr BTC/Surlyn/PP

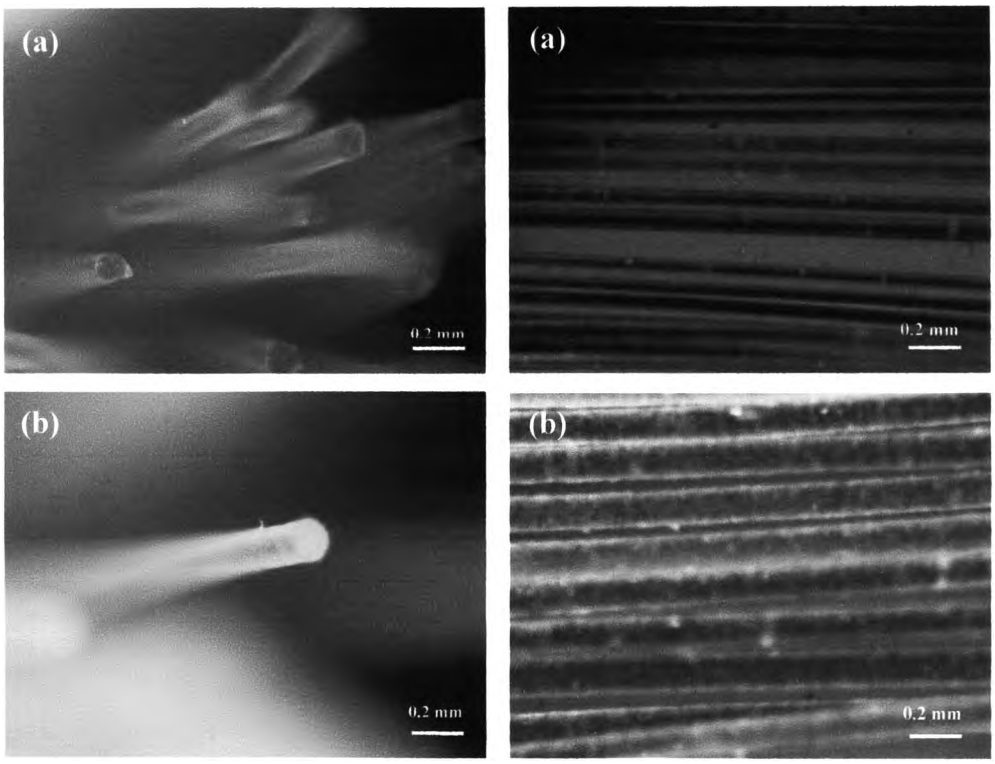

Figure 4.35 Images (120x) of fibers dyed with direct dye (a) PP (b) 5 phr BTC/Surlyn/PP

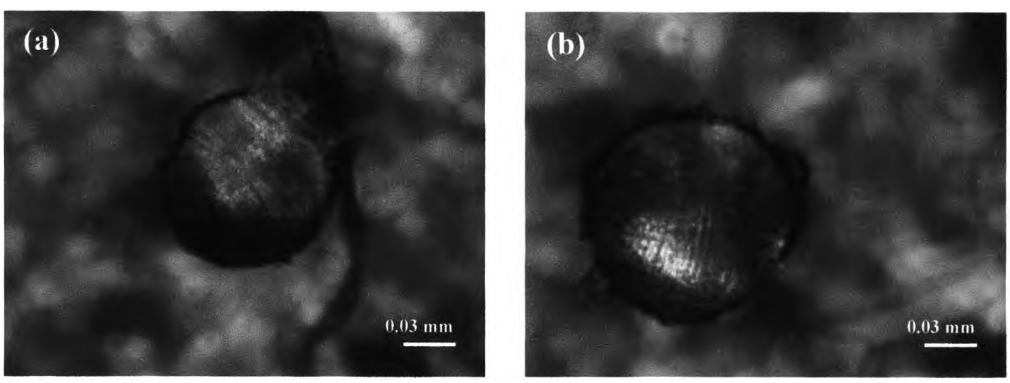

Figure 4.36 Images (600x) of fiber cross-section dyed with direct dye (a) PP (b) 5 phr BTC/Surlyn/PP

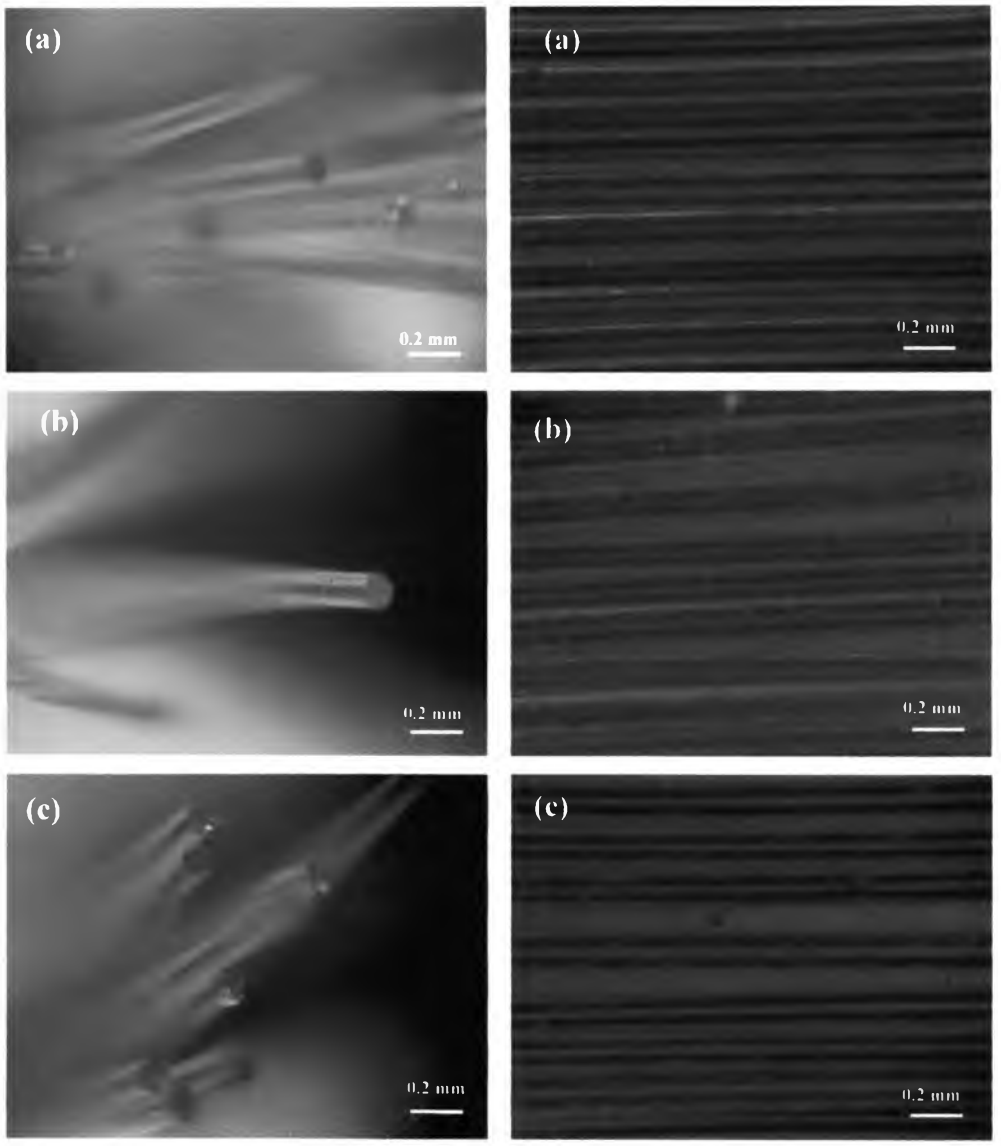

Figure 4.37 Images (120x) of fibers dyed with disperse dye (a) PP (b) 6 phr Surlyn/PP (c) 15 phr PP-g-MAH/PP

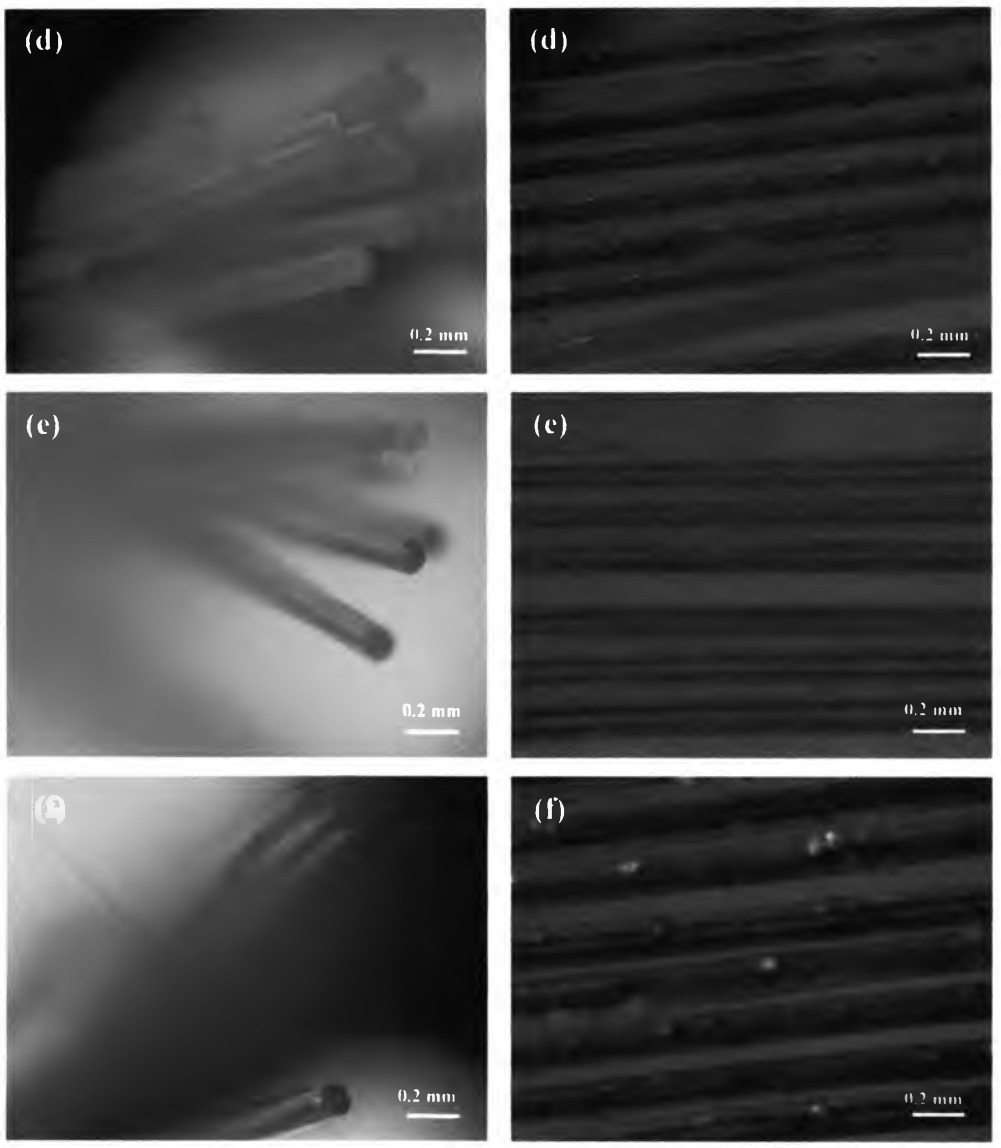

Figure 4.38 Images (120x) of fibers dyed with disperse dye (d) 5 phr BTC/Surlyn/PP (e) 5 phr DOEM/Surlyn/PP (f) 5 phr BTC/PP-g-MAH/PP

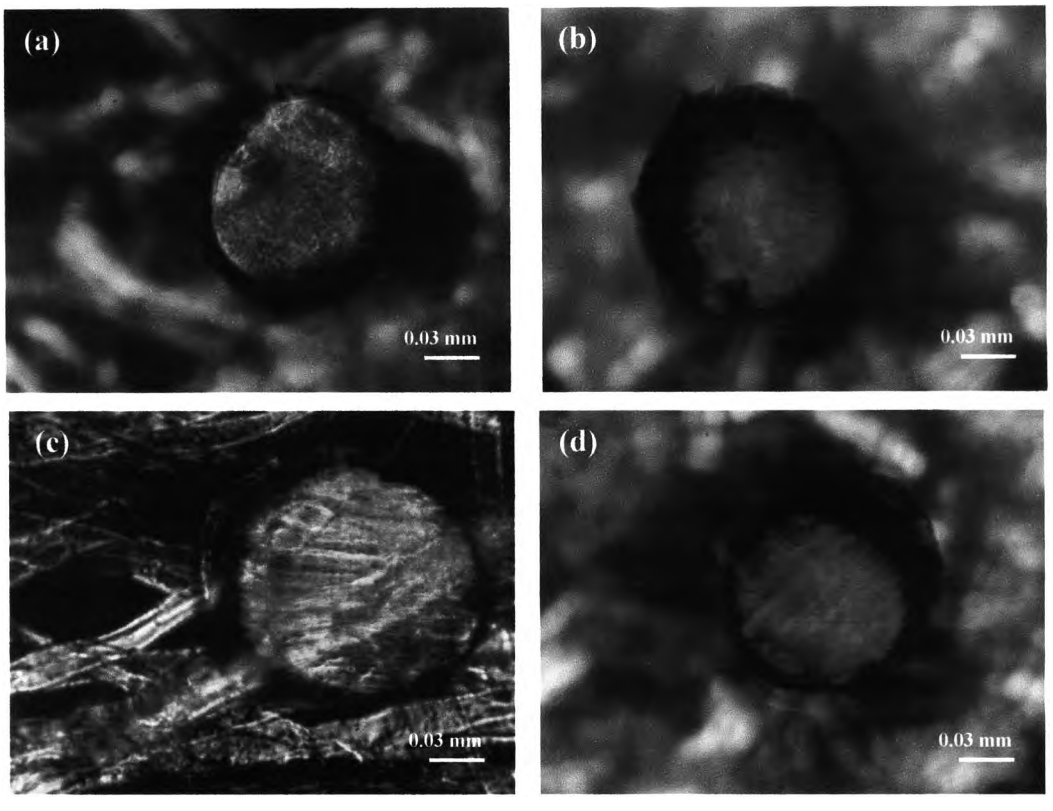

Figure 4.39 Images (600x) of fiber cross-section dyed with disperse dye (a) PP (b) 5 phr BTC/Surlyn/PP (c) 5 phr DOEM/Surlyn/PP (d) 5 phr BTC/PP-g-MAH/PP

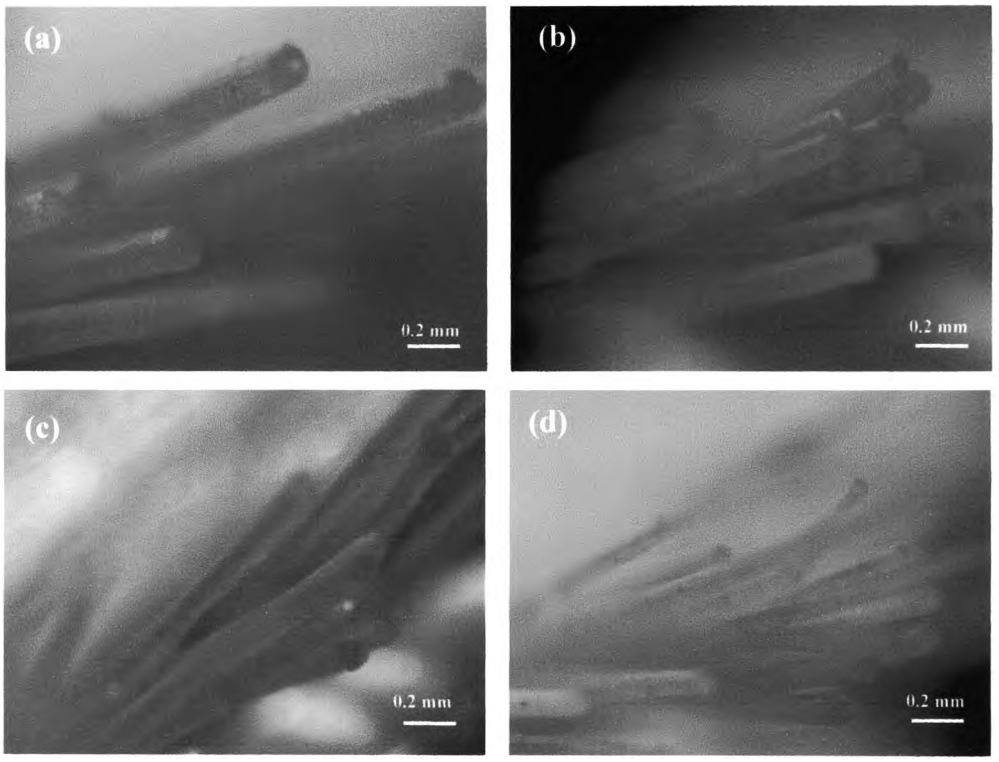

Figure 4.40 Images (120x) of 5 phr BTC/Surlyn/PP fibers dyed with disperse dye and extruded with different draw ratio (x1000) (a) 15.3 (b) 26.5 (c) 36.6 (d) 47.6

4.4.5 Wash Fastness Properties

Wash fastness of the dyed fiber were tested using procedure suggested in ISO 105 C01-C03. The wash fastness of BTC/PP nanocomposite fibers dyed with disperse dye were moderate to good. Due to disperse dye can be absorbed into the fiber not only on the fiber surface but also inside the fiber (Fig. 4.38). Whereas, wash fastness of this kind of fiber dyed with othertypes of dye (acid, basic, and direct dyed) are poor. DOEM/PP nanocomposite fibers dyed with disperse dye show good wash fastness properties but poor wash fastness properties when dyed with acid dye (Table 4.12).

Table 4.12 Wash fastness properties of fibers

Samples	Dyes	Wash fastness
PP	Disperse	4
6 phr Surlyn	Disperse	4-5
15 phr PP-g-MAH	Disperse	4-5
3 phr BTC/Sur/PP	Disperse	3-4
7 phr BTC/Sur/PP	Disperse	4
5 phr BTC/PP-g-MAH/PP	Disperse	4-5
5 phr BTC/Sur/PP	Disperse	4
	Acid	1-2
	Basic	1-2
	Direct	1-2
5 phr DOEM/Sur/PP	Disperse	4-5
	Acid	3-4

CONCLUSIONS

Incorporation of organoclay into polypropylene fiber resulted in an improvement of the thermal, mechanical, and dyeing properties of the fiber. Organoclay can act as the active sites in non polar structure of polypropylene for dye molecules to attach. When the organoclay content increased, the dye absorption also increased. Structure of surfactant used to modify nanoclay also played an important role on the dyeability of the fiber because most of dye molecules consist of aromatic structure so it has more efficient to interact with aromatic groups of BTC-organoclay than the polar and ester groups of DOEM–organoclay. Fiber extruded with higher draw ratios resulted in the higher crystallinity, orientation, and rougher surface morphology that affected the dyeing properties of fibers. Fiber with higher crystallinity and orientation caused for dye molecules to be more difficult to penetrate into the fiber resulted in the reduction of dyeability. On the other hand, the greater surface roughness led to better dye absorption due to the flaws and grooves on the fiber can act as the channels to enter into the fiber easily. The result also shown that the dyeability decreased as the draw ratio increased. It was indicated that the effect from crystallinity and orientation was more significant than effect from surface roughness on the dyeability. Although acid dye shown good dyeing properties due to the ionic force between dye can interact with cationic surfactant of

organoclay, only small amount of dyes can penetrated inside the fiber resulted in the poor wash fastness. Disperse dye was found to be the best dye for this fiber because it can be absorbed not only on the fiber surface but also inside the fiber by hydrophobic interaction and Van der Waals force. In addition, it also gave the good wash fastness properties.

4.6 ACKNOWLEDGEMENT

This work is partially funded by the National Research Council of Thailand (NRCT) and Rachadapisek Sompoch Endowment for Research Unit, Chulalongkorn University. The author is grateful for the partial scholarship and partial funding of the thesis work provided by the National Excellent Center for Petroleum, Petrochemicals, and Advanced Materials, Thailand. The authors would like to thank Thai Nippon Chemical Industry Co, Ltd., for providing the raw clay for use throughout this research.

4.7 REFERENCES

[1] V.B., Gupta, and V.K., Kothari. (1997). Manufactured Fibre Technology. London: Chapman&Hall.

[2] Sara, J.K., and Anna, L.L. (1997). Textiles 8th edition. Ohio: Merrill.

[3] Suprakras, S.R., and Mosto; B. (2005). Biodegradable polymers and their layered silicate nanocomposites: In greening the 21st century materials world. Progress in Materials Science, 50, 962-1079.

[4] Yukio, M., Satoshi, N., and Hidetoshi, K. (1997). Dyeable polypropylene fiber. Journal of Applied Polymer Science, 63, 133-135.

[5] M., Muskatell, L., Utevski, M., Shenker, S., Daren, M., Peled, and Y., Charit. (1997). Flame retardant polypropylene fibers with good dyeability. Journal of Applied Polymer Science, 64, 601-606.

[6] Bhuvanesh, G., and Clara, P., (1999). Modified polypropylene fibers with enhance moisture absorption and disperse dyeability. Journal of Applied Polymer Science, 73, 2293-2297.

[7] Chengbing, Y., Meifang, Z., Xingyuan, S., and Yanmo, C. (2001). Study on dyeable polypropylene fiber and its properties. Journal of Applied Polymer Science, 82, 3172-3176.

[8] Xin, H., Hao, Y., Meifang, Z., and Yanmo, C. (2005). Journal of Applied Polymer Science, 96, 2360-2366.

[9] Ali, R.T.B., A.M., Shoushtari, R.M.A., Malek, M., Abdous. (2004). Effect of chemical oxidation treatment on dyeability of polypropylene. Dyes and pigments, 63, 95-100.

[10] Ozlem, C., and Demet, B., (2001). Adsorption of some textile dyes by hexadecyltrimethylammonium bentonite. Turk Journal Chem, 25, 193-200.

[11] Piyamaporn, J., Jakrit, A., and Ratanawan, W.K. (2005). Uptake of cationic and azo dyes by montmorillonite in batch and column systems. Thammasat Int. J. Sc. Tech., 10, 47-56.

[12] P., Baskaralingam, M., Pulikesi, D., Elango, V., Ramamurthi, and S., Sivanesan. (2006). Adsorption of acid dye onto organobentonite. Journal of Harzardous Materials, B128, 138-144.

[13] Yiqi, Y., and Shinyoung, H. (2005). Nanoclay and modified nanoclay as sorbents for anionic, cationic and nonionic dyes. Textile Res. J., 75(8), 622-627.

[14] M., Joshi, V., Viswanathan. (2006). High-performance filaments from compatibilized polypropylene/clay nanocomposites. Journal of Applied Polymer Science, 102, 2164-2174.

[15] Xinqin, Z., Mingshu, Y., Ying, Z., Shimin, Z., Xia, D., Xuexin, L., Dujin, W., and Duanfu, X. (2004). Polypropylene/montmorillonite composites and their application in hybrid fiber preparation by melt-spinning. Journal of Applied Polymer Science, 92, 552-558.

[16] Quingo, F., Samuel, C.U., Alton, R.W., and Yassir, S.D. (2001). Dyeable polypropylene via nanotechnology. AR. National Textile Center. http://www.ntcresearch.org/pdfrpts/AnRp01/C01-D20-A1.pdf

[17] Quingo, F., Samuel, C.U., Alton, R.W., and Yassir, S.D., and Gopinath, M. (2002). Dyeable polypropylene via nanotechnology. AR. National Textile Center. http://www.ntcresearch.org/pdfrpts/AnRp02/C01-MD20-A2.pdf

[18] Quingo, F., Samuel, C.U., Alton, R.W., and Yassir, S.D., and Gopinath, M. (2002). Dyeable polypropylene via nanotechnology. AR. National Textile Center.

[19] Sakkarin T. (2007). Polypropylene/organoclay nanocomposites for pH-sensitive packaging. M.S. Thesis, The Petroleum and Petrochemical Collage, Chulalongkorn University, Bangkok, Thailand.

[20] Morales, E., and White J. R. (1988). J. of Mater. Sci., **23**, 3612-3622.